UNIVERSITY OF TARTU
Faculty of Science and Technology
Institute of Technology

Ali Jafarov

Deciphering the two dominant interfacial types of tryptophans in photosynthetic membrane proteins using PFAST

Master's Thesis (30 ECTS)
Curriculum Bioengineering

Supervisor(s):
Ass. Prof. Kõu Timpmann
Prof. Arvi Freiberg

Tartu 2022

Deciphering the two dominant interfacial types of tryptophans in photosynthetic membrane proteins using PFAST

Abstract:

Photosynthesis nourishes nearly all life on Earth. Therefore, a deeper understanding of how sunlight is converted into stored chemical energy presents a fundamental and continuing challenge for basic scientific research. The explosive global demand for sustainable energy, the increasing uncertainty of climate change, and the waning worldwide food and water security have increased research's practical value and urgency in this area. Much of the basic science concerning visible-range light harvesting, energy transfer, and subsequent charge separation in reaction centres is now generally considered to be well understood. However, essential questions and controversies remain, such as the protein matrix's structural and dynamical role in governing these processes' energetics, kinetics, and directionality, facilitated mainly by pigment molecules such as chlorophylls and carotenoids.

Present work is the first attempt to cover this critical gap of knowledge. Since proteins are spectroscopically accessible only in the ultraviolet (UV) spectral range, achieving this goal requires, apart from significant mental efforts, also important development of an experimental basis. Observing the response of the collective protein network via the Trp absorption and fluorescence and simultaneously the specific pigment sites via the respective pigment probe signals in a single spectrum is a promising new approach for the research.

Keywords: *photosynthesis, purple bacteria, light-harvesting complexes, fluorescence, spectroscopy, tryptophane*

CERCS: P260 condensed matter: electronic structure, electrical, magnetic and optical properties, superconductors, magnetic resonance, relaxation, spectroscopy; T490 Biotechnology

Kahe domineeriva trüptofaani liidese tüübi dešifreerimine fotosünteetilistes membraanivalkudes PFAST-i abil

Lühikokkuvõte:

Fotosüntees toidab peaaegu kogu elu Maal. Seetõttu kujutab põhjalikumat arusaamist, kuidas päikesevalgus muundatakse salvestatud keemiliseks energiaks, fundamentaalseks ja jätkuvaks väljakutseks fundamentaalsetele teadusuuringutele. Ülemaailmne plahvatuslik nõudlus säästva energia järele, kliimamuutuste kasvav ebakindlus ning ülemaailmne toidu- ja veejulgeoleku kahanemine on suurendanud teadusuuringute praktilist väärtust ja kiireloomulisust selles valdkonnas. Suur osa põhiteadusest, mis puudutab nähtava ulatusega valguse kogumist, energiaülekannet ja sellele järgnevat laengu eraldamist reaktsioonikeskustes, on nüüdseks üldiselt hästi mõistetav. Siiski jäävad alles olulised küsimused ja vaidlused, nagu valgumaatriksi struktuurne ja dünaamiline roll nende protsesside energeetika, kineetika ja suunatavuse reguleerimisel, mida soodustavad peamiselt pigmendimolekulid nagu klorofüllid ja karotenoidid.

Käesolev töö on esimene katse katta seda kriitilist lünka teadmistes. Kuna valgud on spektroskoopiliselt ligipääsetavad vaid ultraviolettkiirguse (UV) spektrivahemikus, nõuab selle eesmärgi saavutamine peale märkimisväärsete vaimsete pingutuste ka olulist eksperimentaalse baasi arendamist. Kollektiivse valguvõrgu reaktsiooni jälgimine Trp absorptsiooni ja fluorestsentsi kaudu ning samaaegselt spetsiifiliste pigmendikohtade jälgimine vastavate pigmendisondi signaalide kaudu ühes spektris on paljutõotav uus lähenemisviis, mis võib pakkuda põnevaid tulemusi.

Võtmesõnad*: fotosüntees, lillad bakterid, valgust koguvad kompleksid, fluorestsents, spektroskoopia, trüptofaan*

CERCS: P260 Tahke aine: elektrooniline struktuur, elektrilised, magneetilised ja optilised omadused, ülijuhtivus, magnetresonants, spektroskoopia; T490 Biotehnoloogia

TABLE OF CONTENT

	P.
TERMS, ABBREVIATIONS AND NOTATIONS	5
INTRODUCTION	6
1. LITERATURE REVIEW	7
1.1. PHOTOSYNTHESIS IS A FUNDAMENTAL PROCESS OF LIFE	7
1.2. TYPES OF THE PHOTOSYNTHETIC PROCESSES	8
1.3. PURPLE SULFUR BACTERIA	9
1.4. PHOTOSYNTHESIS OF PURPLE BACTERIA	11
1.4.1. BACTERIAL LH COMPLEXES	12
1.4.2. LIGHT-HARVESTING COMPLEX II	14
1.4.3. LIGHT-HARVESTING COMPLEX I	15
1.4.4. ENERGY TRANSFER	15
1.5. SPECTROSCOPY APPLICATION IN PHOTOSYNTHETIC RESEARCH	17
2. AIMS OF THE THESIS	21
3. EXPERIMENTAL PART	22
3.1. MATERIALS AND METHODS	22
3.1.1. MATERIALS	22
3.1.2. METHODS	23
3.1.2.1. UV-VISIBLE ABSORPTION	23
3.1.2.2. SPECTROMETRY	25
3.1.2.3. DATA ANALYSIS	26
3.1.2.3.1. SIMS DECOMPOSITION ALGORITHMS	26
3.2. RESULTS	28
3.2.1. UV-VIS ABSORPTION SPECTROSCOPY MEASUREMENTS	28
3.2.2. EMISSION SPECTRA OF LH2 COMPLEXES FROM DIFFERENT BACTERIA	29
3.2.3. FLUORESCENCE CORRELATION ANALYSIS USING PFAST	30
3.3. DISCUSSION	35
SUMMARY	36
REFERENCES	37
APPENDIX 1	44
NON-EXCLUSIVE LICENCE TO REPRODUCE THESIS AND MAKE THESIS PUBLIC	45

TERMS, ABBREVIATIONS AND NOTATIONS

3HPB – bicycle of 3-hydroxypropionate

BChl – Bacteriochlorophyll

CBB – Calvin-Benson-Basham cycle

Chl – Chlorophyll

ICM – intracytoplasmic membrane

J – joule

LH – Light-harvesting complex

OEC – The oxygen-evolving complex

PFAST – protein fluorescence and structure toolkit

Phe – phenylalanine

PS – photosystem

ps – picoseconds

RC – reaction centre

rTCA – the reverse cycle of tricarboxylic acids

Trp – tryptophan

Tyr – tyrosine

UV – ultraviolett

WT – wild type

E. – Ectothiorhodospira

R. – Rhodoblastus

Rb. – Rodobacter

Rba. – Rhodobacter

Rps. – Rhodopseudomonas

T. – Thermochtomatium

INTRODUCTION

Photosynthesis is a unique process in the Earth's biosphere, which is a source of organic matter and energy for most living organisms. Its study is traditional for plant physiology and biochemistry, but even now, in the postgenomic or epigenetic era, this process leaves many secrets. Active molecular-biological, biophysical, and molecular-genetic research of bio- and artificial systems for various levels of complexity involved in the process of photosynthesis is being carried out. At the same time, the popularity of studies of photosynthesis processes on a global scale is growing due to its exceptional role in ecosystems and the biosphere (Montalti et al., 2006; Stirbet et al., 2020).

Various types of photosynthesis are known, except for the most common oxygenic (with the release of oxygen). It has been established that one of the first organisms capable of photosynthesis is an anoxygenic phototrophic bacterium (APB), which has developed under the extreme conditions of the ancient Earth (Blankenship et al., 2007). Therefore, an interesting group in this aspect is the phototrophic purple bacteria, which are widely distributed in nature. They have an anoxygenic photosynthesis process, offering many options to explore due to their diversity.

The existing concepts of the structural features of the photosynthetic apparatus in purple bacteria do not answer fundamental questions and require additional research. Membrane protein complexes of these bacterial groups are naturally constructed in such a way that amino acids are arranged in an ordered manner. For example, in bacterium *Rba. sphaeroides* tryptophan residues are located in the cytoplasmic and periplasmic parts of the protein, while it is absent in the transmembrane helix part, which leads us to the question of involvement not only as a structural component but also as a functionally active one (Timpmann et al., 2021). In particular, a topical issue is to study the possibility of separating signals from several tryptophan residues within a protein.

This work carried out spectral analysis of photosynthetic light-harvesting complexes of purple bacteria. For this, component analysis of the light-harvesting complexes was performed. After that, the fluorescence of the proteins in LH complexes was measured and integrated into the open-source platform PFAST for decomposition analysis of tryptophan residues. Finally, the protein structures were analysed relative to the decomposed fragments.

1. LITERATURE REVIEW

1.1. PHOTOSYNTHESIS IS A FUNDAMENTAL PROCESS OF LIFE

Photosynthetic plant organisms, with the participation of green pigments of chlorophylls, capture sunlight's unlimited cosmic light energy, assimilating inorganic compounds of terrestrial origin, and creating organic substances with stored energy in chemical bonds. Without exaggeration, the phenomenon of photosynthesis is a perpetual motion machine and the preserver of life (Smashevsky, 2014). It supports almost all alive processes on earth, including the respiratory and nutrition of living creatures, and is involved in human energy consumption as, for example, fossil fuel. Unlike autotrophic organisms, which are capable of capturing the energy of solar radiation and using it to synthesise nutrients, heterotrophs cannot directly use sunlight, which makes them dependent on biomass consumption (Montalti et al., 2006).

In addition, photosynthesis plays the role of an environment-forming factor in the Earth's biosphere, providing gas homeostasis in the atmosphere, absorbing carbon dioxide, which is a product of the respiration of all living organisms, and releasing oxygen necessary for aerobically breathing organisms. Also, the oxygen released maintains an ozone shield that protects from the harmful effects of ultraviolet rays. The latter created the conditions for the emergence of life from the ocean on the Earth's land surface (Galili et al., 2014).

Thus, the photosynthesis of green plants is both a factor and a condition for life on Earth in the literal and figurative sense. Its colossal scale of productivity evidence this. Every year, about 200 billion tons of biomass are formed on Earth due to photosynthesis, equivalent to an energy equal to 3-1021 J. The assimilation of carbon dioxide because of photosynthesis during the year is about 260 billion tons, which is equivalent to 7.8 tons of carbon. This carbon sequestration is compensated by the release of almost the same amount of CO_2 involved in the photosynthesis-respiration cycle (Reddy et al., 2010). And the population of the Earth annually consumes only 1 billion tons of products or about 15-1018 J in the form of organic matter, which is only 0.5 % of all energy stored from the photosynthetic process, including agricultural production. Consequently, almost the entire Earth is a direct or distant result of photosynthesis, which mediates between the inexhaustible energy of the Sun and the whole living world of our planet (Hansen et al., 2005; Smashevsky, 2014).

In connection with the increase in the level of energy consumption (according to various estimates, it will increase by 85 % in 2040 (Jones & Mayfield, 2012; Kumar Maurya et al., 2021)), which will lead to the release of carbon dioxide (CO_2) in the atmosphere, primarily due

to an increase in transport load, there is a need to use phototrophic organisms as alternative energy sources (Serrano-Ruiz & Dumesic, 2011; Hill et al., 2020). The importance of this problem is inexorable, which gives impetus to its development in interdisciplinary aspects.

1.2. TYPES OF THE PHOTOSYNTHETIC PROCESSES

Phototrophic organisms have the ability to convert light energy into the energy of chemical bonds. These organisms use different amounts of pigments (chlorophylls and bacteriochlorophylls) for photochemical processes (Figure 1) (Reinbothe, 1996; Hamilton, 2019).

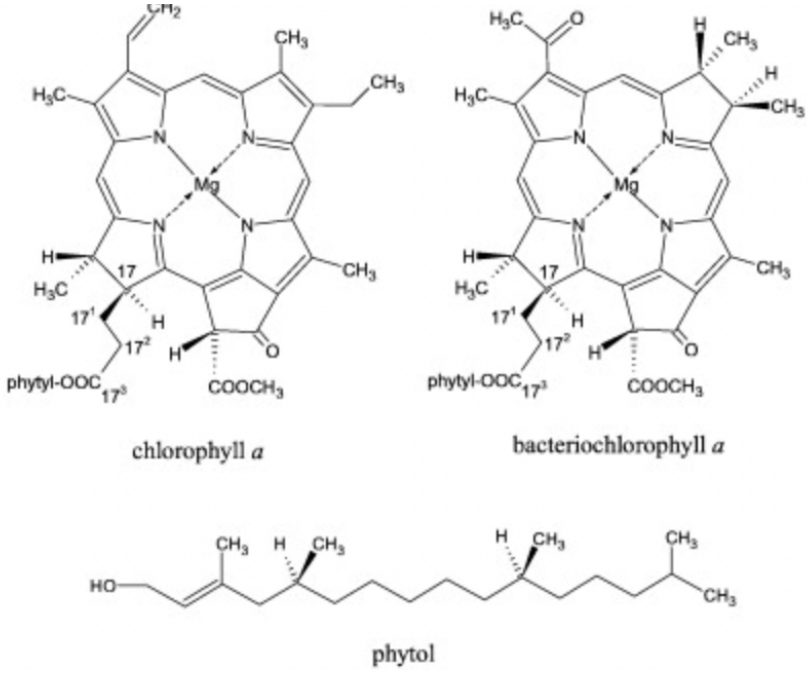

Figure 1. Chlorophyll a (**left**) and bacteriochlorophyll a (**right**). Photosynthetic pigments of organisms with oxygenic photosynthesis (Chl a) and anoxygenic type (BChl a). The molecules have a common structure, the differences are expressed in substitutions around the ring, length, and substitutions on the phytol tail. Bacteriochlorophylls capture the long-wave absorption maximum in the infrared wavelength range (Fiedor et al., 2008)

To date, bacterial groups that are capable of synthesising (bacterio)chlorophylls are known: *Acidobacteria, Chlorobi, Chloroflexi, Cyanobacteria, Firmicutes, Gemmatimonadetes*, and *Proteobacteria* (Figure 2) (Castelle & Banfield, 2018). At the same time, *Cyanobacteria* is the

only truly phototrophic bacterium that has oxygen photosynthesis (involving electrons from water with a by-product of the reaction oxygen). Anoxygenic photosynthesis is the original version of the photosynthetic process, which played a key role in the evolutionary development of oxygen phototrophy (Hamilton, 2019).

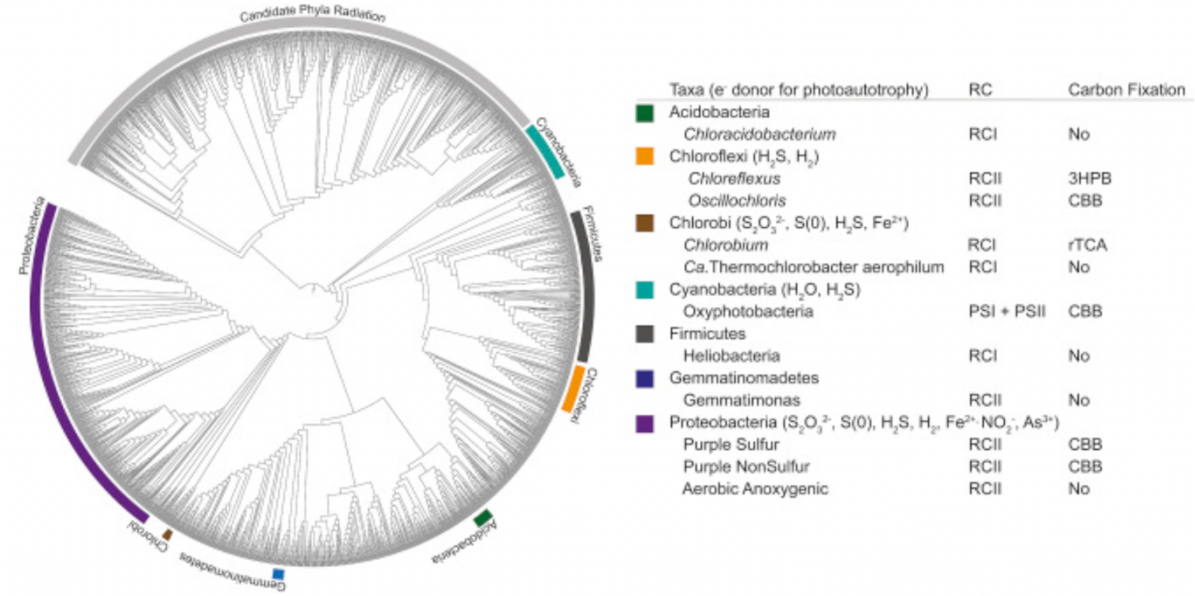

Figure 2. Phylogenetic tree of photosynthetic organisms built based on 14 ribosomal protein sequences of bacteria, archaea and eukaryotes. The reaction centre (RC), the pathways along which carbon fixation occurs, and electron donors are shown. (Brown et al., 2015; Hamilton, 2019)

The anoxygenic photosynthesis pathway releases energy using chemical oxidation-reduction reactions. Thus, organic carbon, Fe^{2+}, H_2, S, HS^-, $S_2O_3^{2-}$, NO^{2-}, and AsO_3^{3-} are precursors in these processes. Bacterial cultures themselves are not always obligate anaerobes, demonstrating tolerance to atmospheric oxygen (Blankenship et al., 2007).

1.3. PURPLE SULFUR BACTERIA

Anoxygenic purple photosynthetic gram-negative bacteria are widely distributed in nature, in aquatic and terrestrial environments. They are found in almost all water reservoirs, as well as in the soil. Their main habitats are fresh and saltwater containing hydrogen sulfide. In stagnant water bodies rich in organic matter, purple bacteria develop in large numbers, forming massive

aggregations. These bacteria carry out photosynthesis by absorbing light with a wavelength of 800 to 900 nm (Milukov, 2007). A description of the main features of this group of microorganisms is noted in Table 1.

Table 1. General properties of anoxygenic purple phototrophic bacteria [1] (adapted from Madigan & Jung, 2009)

Property	Examples
Groups/phylogeny	Purple sulfur bacteria (gammaproteobacteria); purple nonsulfur bacteria (α-or β-proteobacteria)
Major species known	*Allochromatium vinosum* and *Thiocapsa roseopersicina* (purple sulfur bacteria); *Rhodobacter capsulatus*, *Rhodobacter sphaeroides*, *Rhodospirillum rubrum*, and *Rhodopseudomonas palustris* (purple non sulfur bacteria)
Pigments/colour of dense cell suspensions	BChl α or β; major carotenoids include spirilloxanthin, spheroidene, lycopene, and rhodopsin, and their derivatives; cell suspensions purple, purple-red, purple-violet, red, orange, brown, or yellow brown (BChl α-containing species); green or yellow (BChl β-containing species)
Location of pigments in cells	Within intracytoplasmic membranes arranged as membrane vesicles, tubes, bundled tubes, or in stacks resembling lamellae
Absorption maxima of living cells	BChl α-containing species: near 800 nm, and anywhere from 815–960 nm; BChl β-containing species: 835–850 nm and 1010–1040 nm
Electron donors/sulfur globules[2]	H_2S, S, $S_2O_3^{2-}$, H_2, Fe^{2+}; if S is produced from the oxidation of sulfide, the S is stored intracellularly only in certain purple sulfur bacteria
Photoheterotrophy/dark respiratory growth	Purple sulfur bacteria limited on both accounts; purple nonsulfur bacteria typically diverse on both accounts

The photosynthetic pigments of purple bacteria are bacteriochlorophylls and carotenoids. Unlike cyanobacteria, purple bacteria photosynthetic processes under anoxic (without oxygen) conditions, having the ability to conserve energy through photophosphorylation (Madigan & Jung, 2009; Sadi & Firmansyah, 2020; Philippi et al., 2021).

[1] Purple bacteria are a group of gram-negative prokaryotes containing peptidoglycan and a lipopolysaccharide outer membrane. All purple bacteria are gram-negative prokaryotes. All species contain peptidoglycan and an outer membrane containing lipopolysaccharide.
[2] Purple bacteria are characterized by autotrophic growth, using the Calvin cycle as a mechanism for oxygen dioxide fixation.

1.4. PHOTOSYNTHESIS OF PURPLE BACTERIA

For a long time, purple bacteria served as a model organism in the field of photosynthetic light reactions. This is potentially possible with the great diversity of the group and presumably evolutionarily older photosynthetic system (i.e., the progenitor of the plant photosystem (Blankenship et al., 2007)). Purple bacteria have in their structure a bacteriochlorophyll (BChl) special paired reaction centre (RC) of type II (pheophytin-quinone) (Figure 3), which is involved in light-dependent reactions in the membrane (Ogata, 1964; Niederman, 2017).

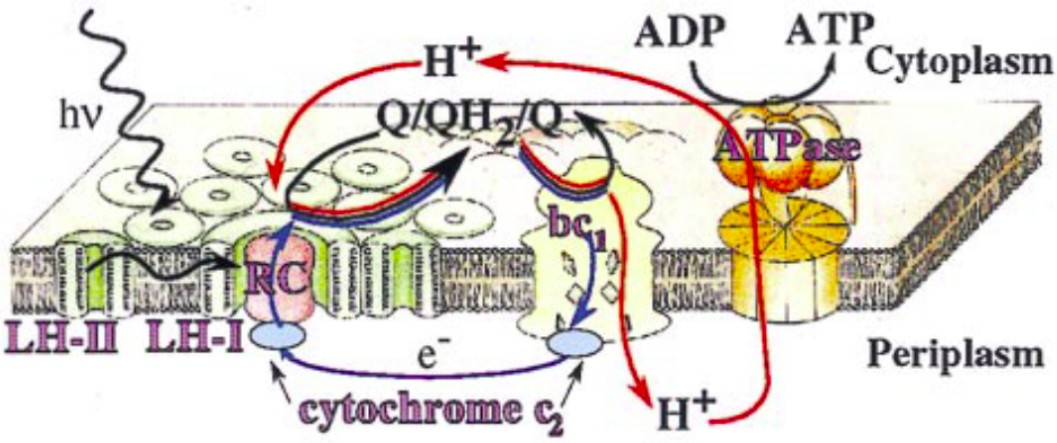

Figure 3. Scheme of electron migration in purple bacteria in the photosynthetic process (anoxygenic type) Light-harvesting antennas are shown as green circles (Hu et al., 1998)

At the same time, purple bacteria do not have an oxygen-evolving complex (OEC), in contrast to phototrophs with an oxygen-type photosynthetic process (Figure 3). Reaction centres of purple bacteria are associated with structures called light-harvesting proteins (the topic is covered in detail in the next chapter 1.4.1. Bacterial LH complexes). The LH2 complex captures light quanta by transferring the excitation to the main antenna LH1, which directs energy to the RC-BChl. Next, the charge gradient decreases on the opposite side of the ICM (Figure 4a). Electron transfer occurs from QA to QB, subsequently resulting in the appearance of a charge on the UQ: cytochrome c2 oxidoreductase (bc1) complex (Figure 4b). Due to the electrochemical concentration gradient, cytochrome c2 is restored to charge offset with bc1, creating a proton gradient (Q-cycle mechanism). Finally, ferrocytochrome c2 completes the electron transfer cycle due to reduction reactions of a pair of photo-oxidised BChl (Francia et al., 2004; Vasilev et al., 2022).

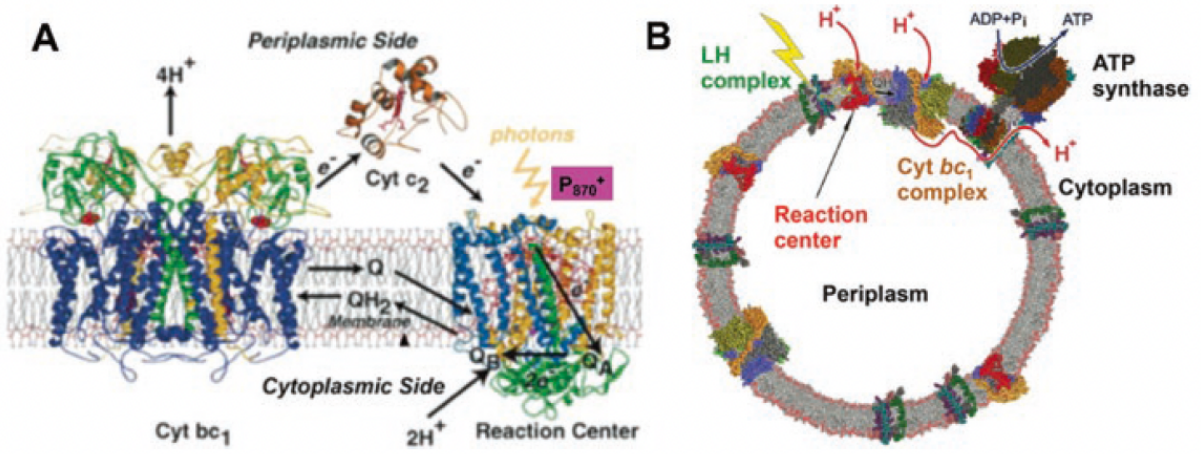

Figure 4. Compositional and dynamic composition of the intracytoplasmic membrane (ICM) electron flow in *Rba. spheroids*. A. Intermembrane charge separation via the quinone/quinol pool, bc1 complex, and cytochrome c2, respectively, resulting in the reduction of P870+, a photooxidised RC-BChl2 special pair. The figure also shows the structures of a bacterial cell's periplasmic and cytoplasmic compartments and their orientation relative to ICM. B. The spheres represent the proteins involved in the process. During the migration of H^+, a gradient is created, resulting in ATP synthesis (Axelrod & Okamura, 2005; Niederman, 2017)

1.4.1. BACTERIAL LH COMPLEXES

One of the most efficient photosynthetic processes is light harvesting. In the case of purple bacteria, this process occurs through membrane pigment-protein complexes called LH complexes (Ferretti et al., 2016). Most photosynthetic antennas are composed of pigment molecules and proteins arranged in specific geometrical clusters, where the proteins form the backbone of the photosynthetic pigments. Due to the unique position, the captured energy can always be taken up by the photoactive pigment. The rate of energy transport between photosynthetic pigments is calculated in picoseconds (ps). Antennas, or peripheral complexes, absorb light from the environment and transfer energy between themselves until it hits the white of the RC.

Two main types of LH complexes are distinguished. The first type is the core antenna LH2, which surrounds the RC itself and is the last link in transmitting power directly. The second primary type is the LH2 peripheral antennas surrounding the LH1-RC complex. The ratio of peripheral and central antennas is controlled by the intensity of the incident light on the host organism and depends on the growth condition. The transfer of light energy absorbed by the

LH2 complex to the LH1 complex occurs in 2-4 ps, and the transfer to RC takes 20-40 ps, provided that the membrane is not affected by external factors (Cogdell et al., 2004; Saer & Blankenship, 2017). Visual comparison of the absorption spectra of the two main light-harvesting complexes purified from *Rba. sphaeroides* is shown in Figure 5.

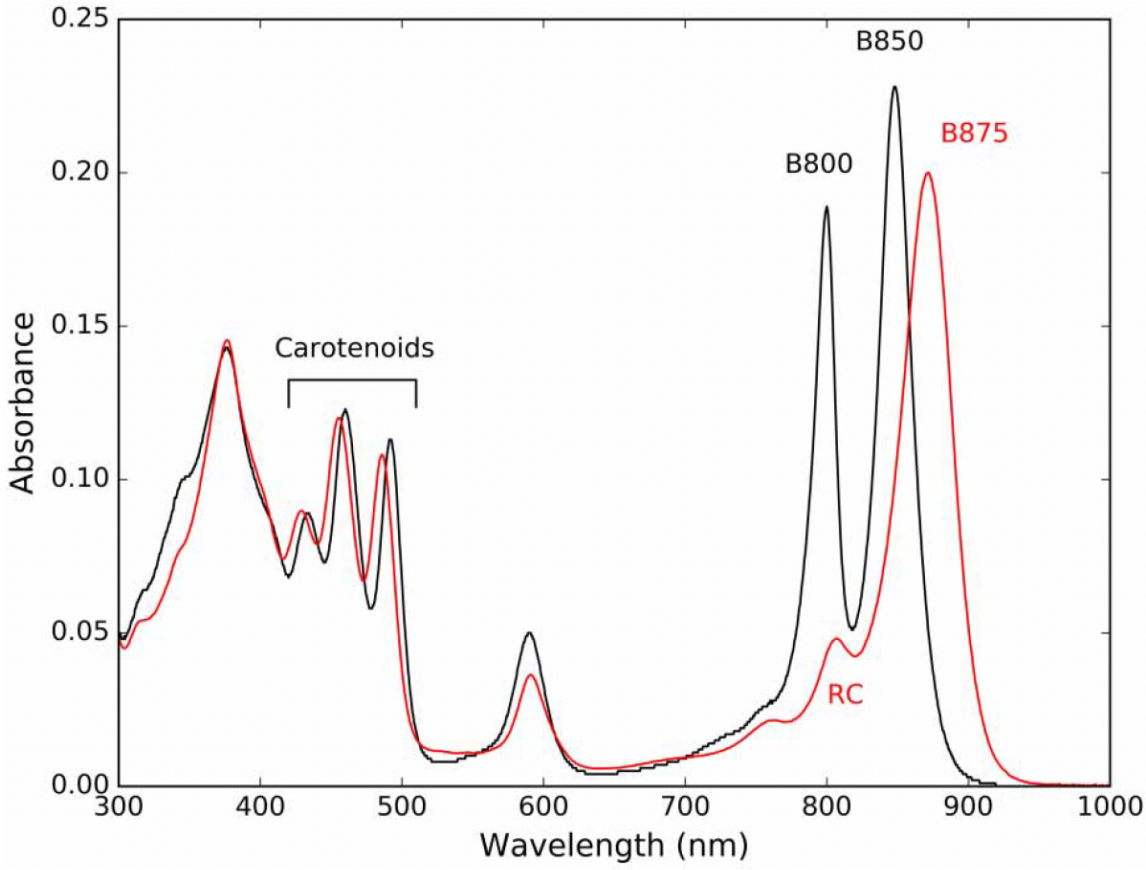

Figure 5. Absorption spectra of light-harvesting complexes isolated from *Rba. sphaeroides* with a genomic mutation leading to the synthesis of neurosporene. The black line indicates LH2 absorption, while the red line shows the LH1–RC complex. Peaks showing the corresponding adsorption are indicated in the graph. The y-axis indicates the level of absorbance, while the x-axis shows the wavelength (nm) (Saer & Blankenship, 2017)

The absorption spectrum of these complexes has visible absorption peaks in the UV and near-infrared regions of the spectrum. Under certain growth conditions, some bacteria also produce other types of peripheral antennas, such as light-harvesting complexes 3 (LH3) and light-harvesting complexes 4 (LH4) (McLuskey et al., 2001).

1.4.2. LIGHT-HARVESTING COMPLEX II

Bacterial LH2 is an octa- or nona-meric ring structure of dimers of repeating pairs of single transmembrane helices of apoproteins α and β and associated BChl a molecules, giving excitation in the range of 800–890 nm and carotenoids. LH complexes from purple bacterium are short, as in the case of LH2 from *Rps. acidophilus* (Figure 6), the α-subunit consists of 53 amino acids and forms the inner part of the ring, while the β-subunit consists of 41 amino acids and forms the outer component. However, this number may vary depending on the host organism (Law et al., 2004). Each polypeptide has one transmembrane helix. The helixes of α-apoproteins lie perpendicular to the membrane plane, while the helices of β-apoproteins are inclined by about 15° relative to it.

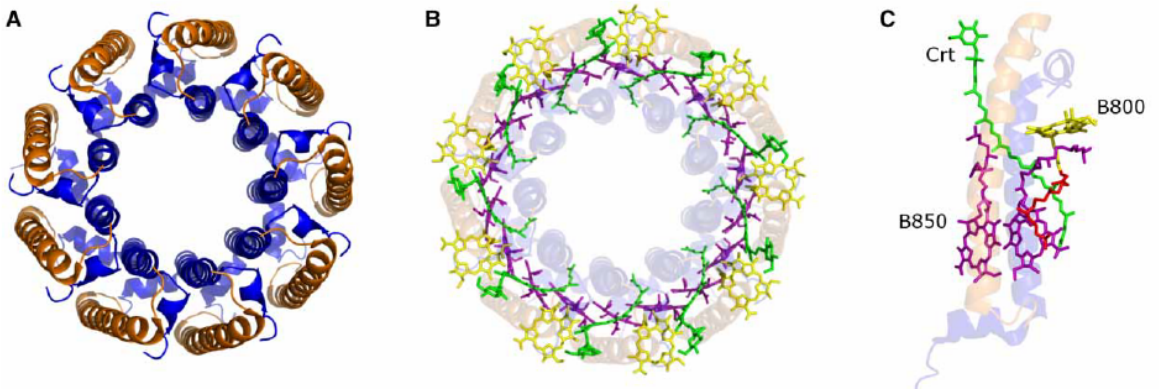

Figure 6. Structural representation of light-harvesting complex 2 from R. acidophilus. A. Orientation of the polypeptides: α (blue) and β (orange) shown perpendicular to the membrane plane; B. Pigments of the complex: BChl B800 (yellow), BChl B850 (violet), carotenoids (green); C. Monomeric unit of the complex with preservation of the colour distribution as in B (Saer & Blankenship, 2017)

The N- and C-termini of both apoproteins fold and interact with each other. The N-terminal region of the transmembrane helix is located on the cytoplasmic side of the membrane, while the C-terminal region is located in its periplasmic part. Between the elements of the integral structure, there are hydrogen bonds formed between significant aromatic residues located at the C-terminus of both apoproteins and BChl (Freer et. al., 1996).

The exciton pigment-pigment and pigment-protein interactions in LH2 give the complex its characteristic redshift of the absorption spectrum in the range from 770 nm in the case of

monomeric BChl a to about 850 nm in LH2. The group of molecules called B800 has Qy absorption bands around 800 nm, and the group called B850 respectively has Qy absorption bands around 850 nm. The bacteriochlorin rings of BChl a B800 lie parallel to the membrane plane. BChl a B800 molecules are monomeric forms separated by approximately 21 Å. In contrast to B850, the central Mg_2 ions of B800 molecules are not linked to the histidine residue but to the carboxylate fragment on the N-terminal amino group of a-Met1 (Cogdell et al., 2004; Papiz et al., 2003).

1.4.3. LIGHT-HARVESTING COMPLEX I

Bacterial LH1 is built with the same modular principle, as the LH2 complex, but in addition, it is associated with RC and forms the LH1-RC complex. The α/β-dimer unit LH1 binds two BChl molecules and one carotenoid. The LH1-RC complexes are used strictly for the photosynthetic apparatus for some bacteria (Figure 7).

Despite numerous studies of the structure of the central complex, its exact form is still a subject of interest for scientists. For example, long-standing studies have shown that LH1 forms a ring structure (Scheuring et al., 2002), but the fact that quinone/quinol moves between RC and the cytochrome bc1 complex via LH1 during electron transfer has raised many questions. As a result of newer scientific studies, LH1-RCs have been found to have an open ring structure for LH1. The transmembrane helix polypeptide prevents the closure of the ring shape (Roszak et al., 2003).

In the case of *Rb. capsulatus* and *Rb. sphaeroides*, this role is presumably performed by the PufX protein. This passage enables the quinone/quinol pathway in the LH1-RC complexes and light-driven electron transfer and photophosphorylation (Siebert et al., 2004) Research on LH1-RC core complex from *Rps. palustris* showed that the LH1 elliptical complex consists of 15 α/β heterodimers, also containing a hole associated with the helix of the W protein (Roszak et al., 2003).

1.4.4. ENERGY TRANSFER

The absorption of light quanta by the photoactive pigment stimulates the transition of the pigment to an excited state, which subsequently leads to one of several possible ways of decay of this excited state. The Forster mechanism describes energy transfer with further capture of

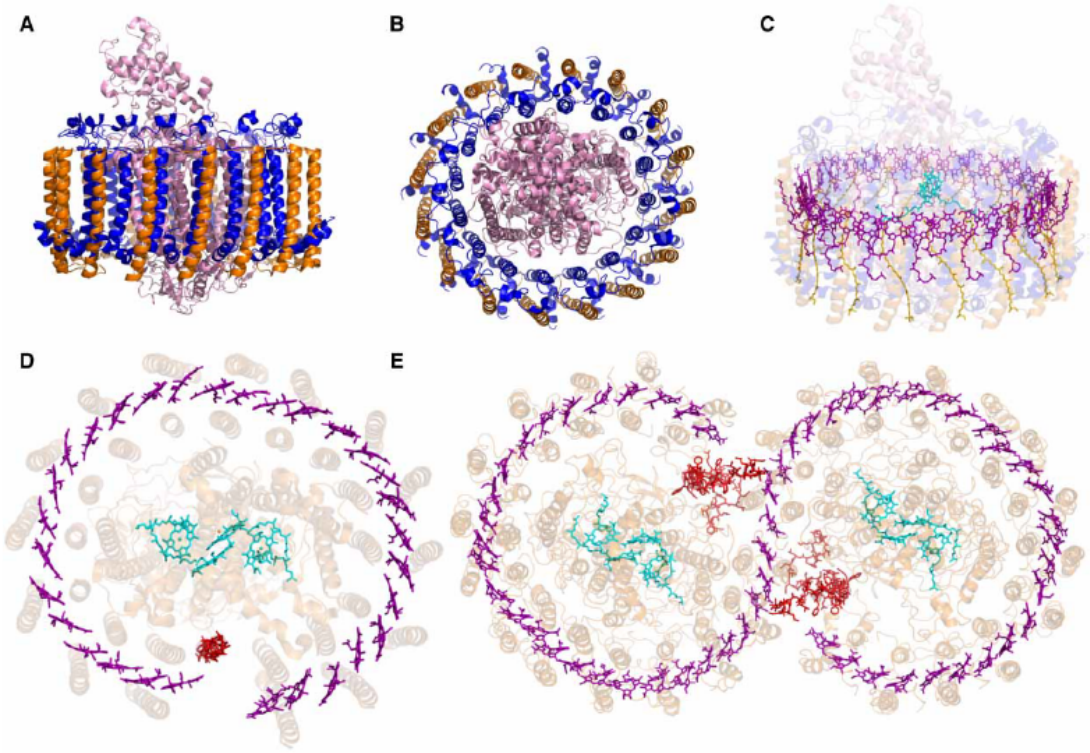

Figure 7. Core complex LH1-RC of purple bacteria. A. High-resolution peptide structure of the *T. tepidum* LH1-RC complex, view parallel to the membrane plane, α-subunit (blue), β-subunit (orange), reaction centre (pink); B. Similar to A, but perpendicular to the membrane plane, periplasm side; C. Pigments of the designated complex BChl B915 (violet), BChl RC (blue), carotenoids (yellow); D. Location of LH1-RC of *Rps. palustris*: core pigments: BChl LH1 (violet), BChl RC (blue), helix W (red), E. Pigments of the S-shaped complex LH1-RC *Rba. sphaeroides*, colour accompaniment as in D, PufX polypeptides in red (Saer & Blankenship, 2017; Tani et al., 2021)

this energy during charge separation within and between LH and RC complexes (Forester T, 1948). However, this process is not always possible because the RC is already in a state with a separate charge. It cannot further convert the excitation energy from the LH complexes. The lifetime of an excited electron after absorption of light by the BChl a molecule is about one ns. Approximately in similar terms, the transfer of energy to RC takes place. In purple bacteria, the direction of energy transfer is from LH2 to LH1 (B800-B850-B875) and then to BChls in RC. Each energy transfer step from the B800 occurs in a lower energy excited state, resulting in a gradient of that same energy (van Amerongen & van Grondelle, 2001).

In the case of LH2 from *Rba. sphaeroides* and *R. acidophilus*, the energy transfer duration between BChls is about 0.7-0.9 ps, while the final transfer in RC takes 30 to 50 ps. The direction of energy transfer is displayed on the absorption spectra of LH2 and LH1 (Figure 8.) (Law et al., 2004).

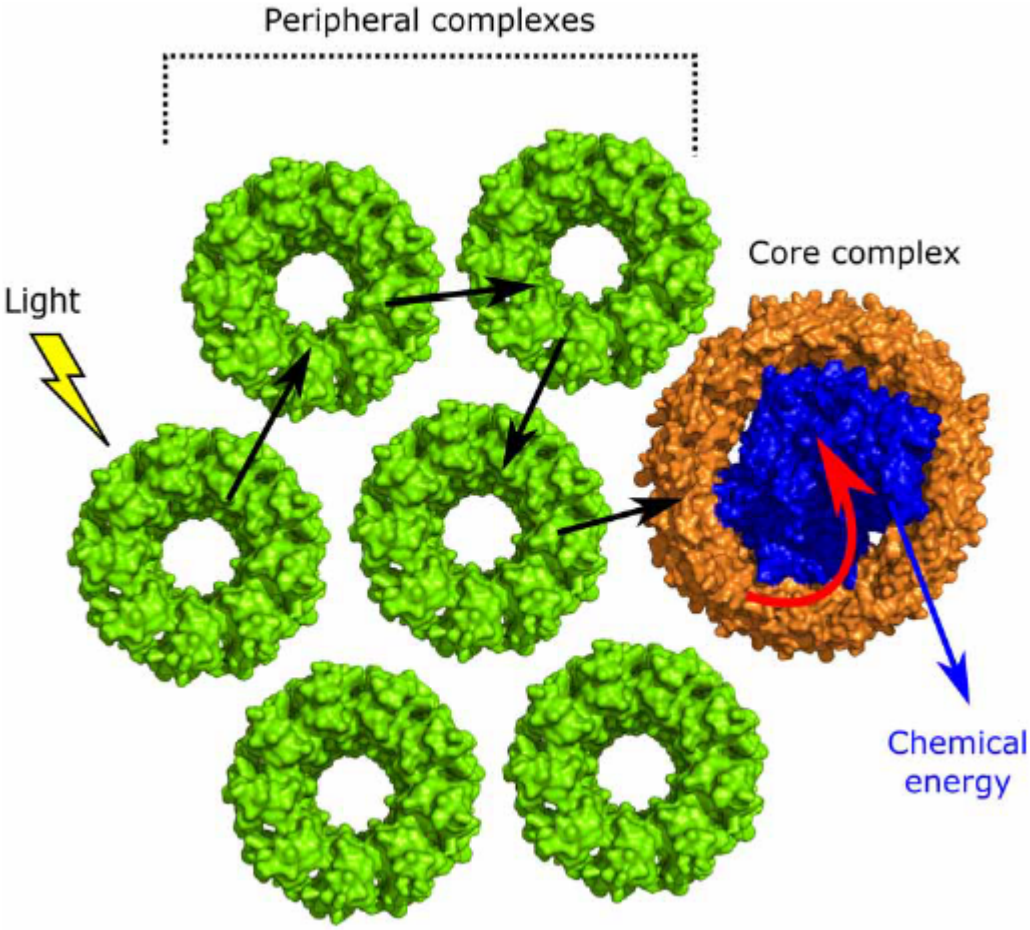

Figure 8. A typical energy transfer pathway in the photosynthetic unit of purple bacteria. Peripheral complexes such as LH2 (green) absorb light energy, mobilizing it across other LH2 complexes until it reaches a core LH1 antenna (orange). Once in the core antenna, energy is trapped by a final transfer step to the reaction centre (blue), at which point the light energy is converted into chemical energy. (Saer & Blankenship, 2017)

1.5. SPECTROSCOPY APPLICATION IN PHOTOSYNTHETIC RESEARCH

Spectroscopy is used to study the structure of atoms and molecules due to many emitted wavelengths. Fluorescence spectroscopy and time-resolved fluorescence are primarily research tools in biochemistry and biophysics and can be used in many disciplines. Fluorescence spectral

data is usually presented as a plot of fluorescence intensity versus wavelength (nm) or wavenumber (cm^{-1}) of emission spectra. Typical fluorescence spectra are shown in Figure 9.

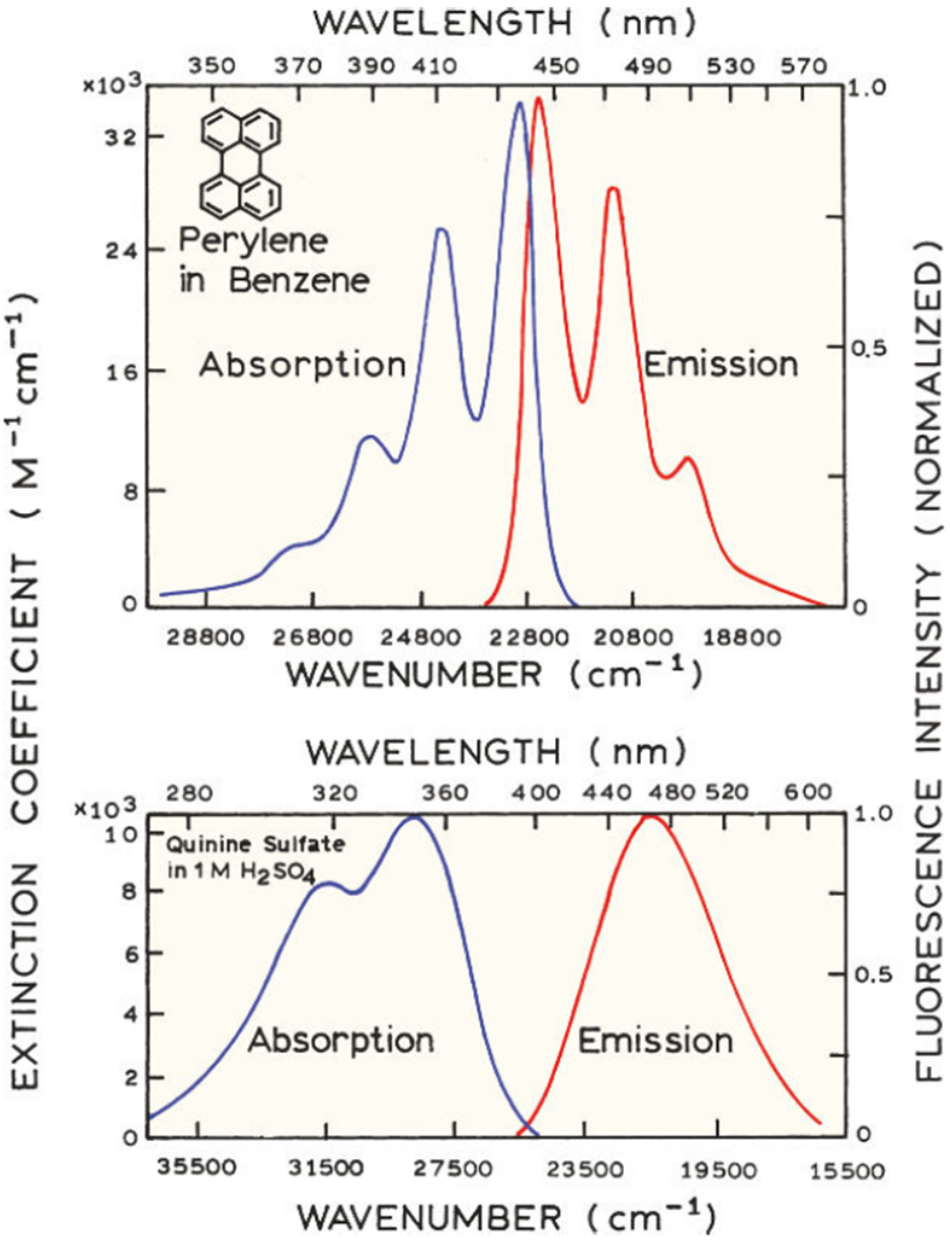

Figure 9. Absorption (blue) and emission (red) spectra of perylene (upper panel) and quinine (lower panel). The chemical structure of both the fluorophore and the solvent strongly influences the emission spectra. Also, the spectra of some compounds can show a significant structure, which is associated with different levels of the vibrational energy of the ground and excited states, while the rest of the compounds lack such structure. (Lakowicz, 2006)

As a means of monitoring refolding transitions caused by chemical denaturants, temperature, changes in pH and pressure, the intrinsic fluorescence of aromatic amino acids in proteins are used. The most widely used fluorescence spectrum is tryptophan, which is sensitive to

perturbations in protein structure. Phenylalanine and tyrosine are less in demand due to low quantum yields (Royer, 1995).

As a starting point for discussing absorption and emission counts, the Jablonski diagram is used (Figure 10), which depicts the different electronic states of molecules and the transitions that occur between these states (Sípoš & Sima, 2020). The founder of the chart is Alexander Jablonski, whose name it bears. The vertical axis of the graph shows an increase in energy in the direction from the bottom to the top. The symbols S_0, S_1, and S_2 denote the ground, first, and second electronic states. The transitions between states and their direction are indicated by arrows. The time of such a transition is approximately 10^{-15} seconds. thus, based on the Franck-Condon principle, we can consider transitions as vertical (Montalti et al., 2006).

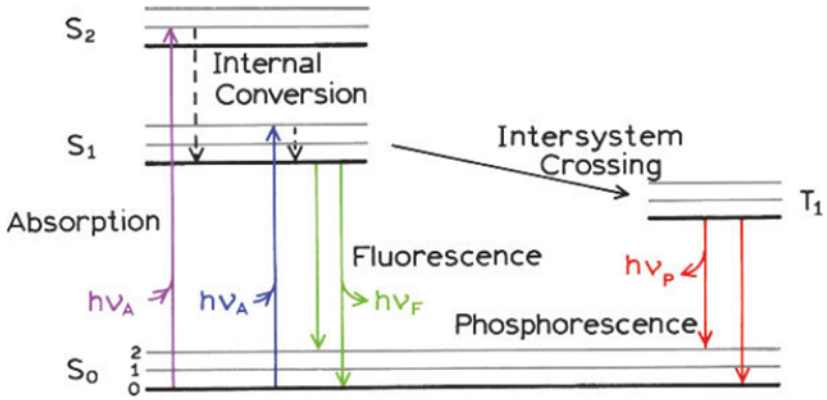

Figure 10. Yablonsky diagram, illustrating energy levels, molecules, and transition rates. Straight lines are radiative transitions, wavy – non-radiative transitions. S_0, S_1, and S_2 are singlet electronic excited states, T_1 is a triplet electronic excited state, and E is energy (Lakowicz, 2006)

The process by which photons are emitted after the transition of the electron from the excited state to the initial state is called fluorescence. A change in the level of the excited state, leading to a deformation of the energy gap, and the environment of tryptophan fluorophores in proteins affect various combinations of interactions that occur in the excited state. Based on this, it can be said that a stationary fluorescence spectrum will reveal what is happening in the environment of tryptophan fluorophores in proteins (Montalti et al., 2006).

The most well studied fluorescent molecules are proteins. Almost all proteins include three amino acid residues, which can directly affect the ultraviolet fluorescence of the protein. These amino acid residues are tryptophan (Trp), tyrosine (Tyr) and phenylalanine (Phe). Since the

maximum absorption of proteins is studied in the region of 280 nm, the Phe luminescence is rarely mentioned in such works due to its relatively low content in the studied molecules. At 280 nm, it is mainly Tyr and Trp that are absorbed; while examining wavelengths above 295 nm (and up to 305 nm), only Trp absorption can be observed for the most part. The emission maximum peak of Trp dissolved in water occurs at a wavelength approximately equal to 348-350 nm (Lakowicz, 2006)

It is important to note that, unlike Tyr and Phe, the spectroscopic properties of Trp are noticeably more complex due to its high sensitivity to the environment, which makes it perfect for observing changes in the protein and its interaction with other molecules, as well as studying the dynamics and physics of micro-environment of the indole fluorophores. The reason for this is a significant redistribution of the electron density in the asymmetric indole ring of the Trp residue after the absorption of photons (Figure 11a). Most of the electron density is lost by the $N\varepsilon_1$ and $C\gamma$ atoms and deposited on the $C\varepsilon_3$, $C\zeta_2$, and $C\delta_2$ atoms of the indole ring upon excitation in the 1La ground fluorescent state (Chen & Barkley, 1998).The blue shift of Trp fluorescence (Figure 11b) towards enhancement of nonpolar media can be explained by the fact that in hydrophobic media the ^1L_b state predominates in the Trp emission since it has the lowest energy compared to the ^1L_a state.

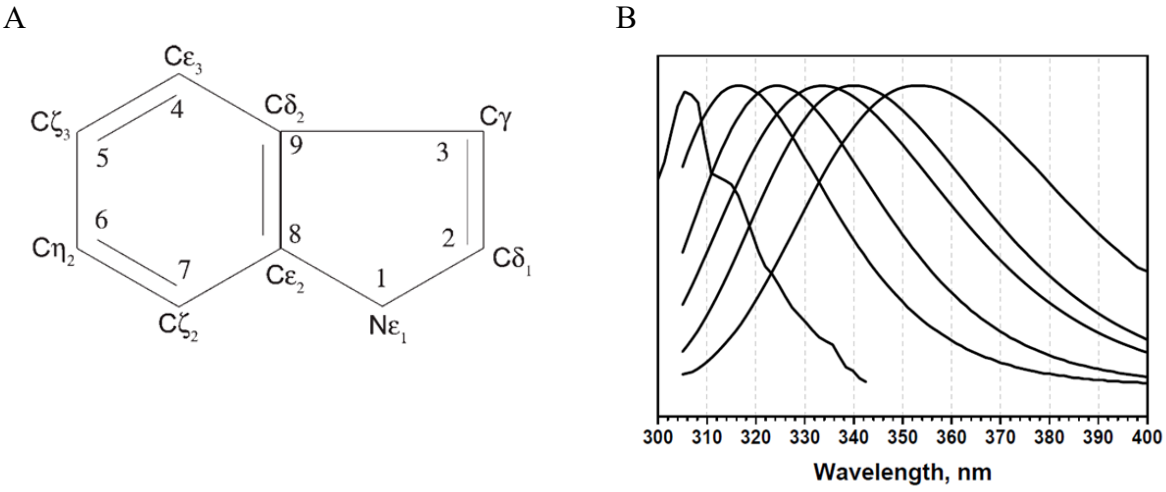

Figure 11. Tryptophane fluorescence. A. Tryptophan indole ring. An aromatic hydroxyl group that absorbs UV radiation and emits a fluorescent signal at various wavelengths, B. Fluorescent emission of tryptophan residues in various protein molecules. Spectral data during fluorescence range from 305 to 355 nm (Hixon & Reshetnyak, 2009)

2. AIMS OF THE THESIS

1. Conduct a component analysis of the composition of the studied light-harvesting complexes of different bacterial cells;
2. Analyse the fluorescence of selected LH complexes using spectroscopy methods for integration into PFAST;
3. Perform decomposition analysis of tryptophan residues from different LH complexes;
4. Conduct an analysis of protein structures in relation to the resulting decomposition analysis.

3. EXPERIMENTAL PART

3.1. MATERIALS AND METHODS

3.1.1. MATERIALS

In this work, we used LH complexes isolated from the membranes of various purple bacteria. To be more precise, LH2 complex from WT *Rba. sphaeroides;* LH2 complex from CrtC$^-$ mutant *Rba. sphaeroides* (M. R. Jones et al., 1992), in which native carotenoid spheroidenone had been replaced by neurosporene; the reference LH2 complex from WT *E. haloalkliphila* and LH3 complex from WT *R. acidophilus* were used. These samples were kindly provided to the Biophysics Laboratory of the University of Tartu through collaborations with the biochemists from Sheffield University (UK). All complexes were purified with a non-denaturing detergent designed to encapsulate the hydrophobic transmembrane part of the LH2 complex. The sequences with Trp positions are shown in Table 2. Also, in Table 3 a more detailed description of the protein subunits is provided, showing the position of tryptophan in protein complexes, indexes of hydrophilicity and level of protein disorder.

Table 2. List of samples used in the work. The bacterial species, strain, and protein sequences of light-harvesting complexes are indicated. Tryptophan position highlighted in yellow

Bacteria	*Rhodobacter sphaeroides*	*Ectothiorhodospira haloalkaliphila*	*Rhodoblastus acidophilus*
Type	WT LH2, neurosporene LH2	WT, car-less	WT
Description	LH2 B-800/850 7PBW	LH2 B-800/8506 Q53	LH3 B-800/820 1IJD
Alpha chain	MTNGKIWLVVKPTV GVPLFLSAAVIASVV IHAAVLTTTTWLPA YYQGSAA	MSEYRPSRPSNPRDD WKLWLVVNPGTWLI PLLITFLATALIVHSFV FTHEAYNPLTYEVSE	MNQGKIWTVVPP AFGLPLMLGAVAI TALLVHAAVLTH TTWYAAFLQGGV KKAA
Beta chain	LNKVWPSGLTVAEA EEVHKQLILGTRVFG GMALIAHFLAAAAT PWLG	MENSISGLTEEQAKEF HEQFKVVFTTFVVLA AAAHFLVFLWRPWF	AEVLTSEQAEELH KHVIDGTRVFLVI AAIAHFLAFTLTP WLH

The concentrated samples were stored at −78 °C in a deep freezer. After, they were diluted in 10 mM Tris-HCl pH 7.5 buffer (200 mM Tris pH 7.5), which contained 1 % β-OG detergent to prevent aggregation. Once in the cuvette, samples were degassed for 1 min using Ultrasonic Cleaner (Cole-Parmer).

In addition, 20 mM HEPES pH 7.5 (400 mM HEPES pH 7.5, 20 % b β-OG, MQ water), 10mM MES pH 6.5 (300 mM MES pH 6.5, 20% β-OG, MQ water) and 10 mM TRIS-MES pH 7 buffer with 1% β-OG (400 mM Tris pH 7.8, 300 mM MES pH 6.5, 20 % β-OG, MQ water) were checked. However, due to their high signal in the UV region, they were excluded from work.

Table 3. Position of the tryptophan residue in the proteins of the light-harvesting subunits of the bacterial complex. The indexes of hydropathy are given (summarised from RCSD PDB database). With a symbol "*" the transmembrane position of Trp is labelled

Bacterium	Protein alpha chain	Hydropathy index	Protein beta chain	Hydropathy index
Rhodobacter sphaeroides	Trp7	0.46	Trp5	0.08
	Trp40	-0.11	Trp45	0
Rhodoblastus acidophilus	Trp7	0.21	Trp40	0
	Trp40	-0.12		
Ectothiorhodospira haloalkaliphila	Trp16	-1.24	Trp41*	1.06
	Trp19	0.37		
	Trp27*	0.38	Trp44	0

3.1.2. METHODS

3.1.2.1. UV-VISIBLE ABSORPTION SPECTROSCOPY

Absorption spectroscopy is often used to determine the concentration of absorbing particles in solutions. In turn, UV-visible spectroscopy is one of the types of absorption spectroscopy in which the molecule absorbs UV-visible light. The result of this approach is the excitation of electrons from lower energy levels to higher ones. The instrument includes a light source (with the ability to generate broadband electromagnetic radiation in the UV-visible spectrum), a dispersion device that splits the broadband radiation into wavelengths, a sample area where light passes/reflects through the sample and detectors for measuring radiation. This list forms the main base of the device. However, it also includes peripheral optical components, such as mirrors, lenses or optical fibres, which serve as light transporters inside the installation. The

Cary 60 UV-Vis Spectrophotometer (Agilent) instrument with a 80 Hz xenon lamp was used to measure absorbance. The schematic of the internal part of the device is shown in Figure 12.

Measurements were carried out from 200 nm to 1000 nm in the ‘medium mode’. Baseline correction was estimated before the start of measurements. Samples in the volume of 600 uL were placed in a 1 mm quartz glass cuvette and fixed in a special holder, after which the measurements started.

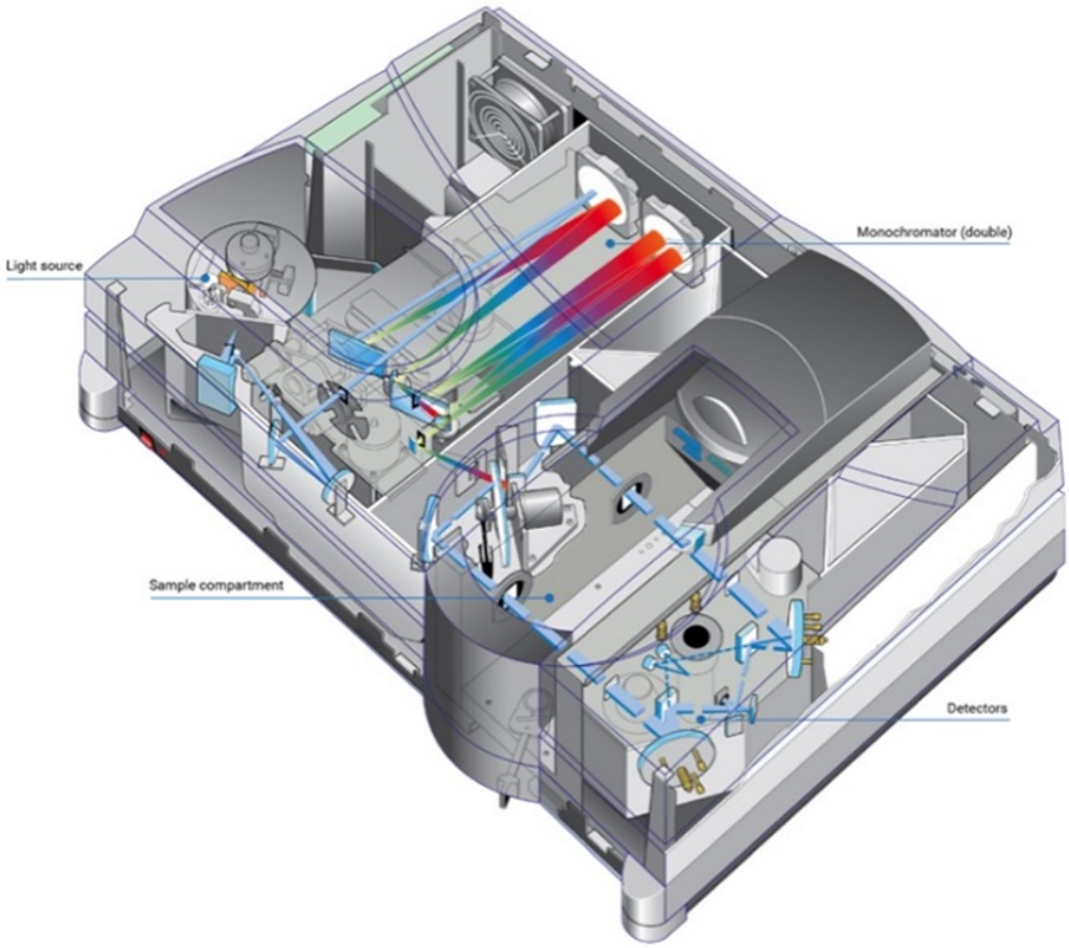

Figure 12. The layout of the elements of the UV-Vis spectrometer. The system is conditionally divided into four blocks: Light source, double Monochromator, Sample compartment and Detector (Determine Protein Concentration..., 2022)

3.1.2.2. SPECTROMETRY

For the emission spectrum measurements, a Chirascan plus CD spectrometer (Applied Photophysics) was used. The schematic diagram of this installation is shown in Figure 13. This system can be separated into three main components: the optical system, the control and connection electronics, and the Chirascan Windows software.

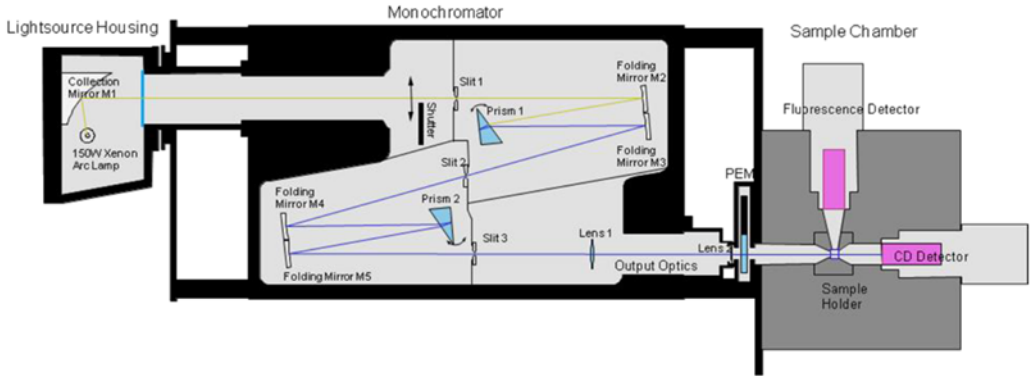

Figure 13. Position of the internal elements of the spectrometer. The yellow and the blue line show the path taken by the light beam from the light source to the sample. The difference in colours occurs since refraction on prism 1, only a particular part of the original beam of light remains. The installation itself is conditionally divided into Lightsource Housing, Monochromator and Sample Chamber (Technical Description of the Chirascan-plus CD Spectrometer, 2008)

The light source was a 150 W xenon lamp. An ellipsoidal focusing mirror was used for maximum efficiency in controlling the light beam. The lamp was air-cooled as standard; however, to reduce the formation of ozone when operating in the UV range, we used nitrogen gas. A monochromator with an F/7 Wollaston split prism and double dispersion and polarisation optics with a wide range of wavelengths were included in the setup. To better separate the light entering the detector by its wavelength and frequency, the Andor Kymera 193i spectrograph (Oxford Instruments) was combined with a spectrometer.

All Trp sample signals were measured from 210 to 300 nm with a step of 2 nm. Due to the complicated and unpredicted nature of the signal in the lowest wavelengths, further data analysis was performed in a region starting from 250 nm. The split width of the setup was 2 nm for all experiments. Accumulation time was set as 20 s due to the low sensitivity of the Trp. Samples were diluted as described in the materials section and piped into a quartz glass cuvette.

3.1.2.3. DATA ANALYSIS

The raw spectra were corrected for background signals (such as Raman scattering) of buffer solvent and for the spectral sensitivity of the setup. Selected spectral bands were characterised by their maximum position, width, and integral intensity. Obtained data were analysed using Origin curve-fitting algorithms (Microcal Software, Inc.).

In the second stage of data analysis, PFAST (Protein Fluorescence and Structure Toolkit) was used to decompose protein Trp fluorescence spectra into spectral components of individual neighbour Trp residues with energy transfer between the Trp within clusters. For each decomposition analysis, one fluorescence spectra were under respect. Finally, three possible component contributions were generated, and these spectral components were assigned to one of five spectral-structural classes. Simulated spectra were also characterised by their maximum position, width, and integral intensity, and then comparative analyses for different samples were performed.

3.1.2.3.1. SIMS decomposition algorithms

PFAST is an open-source platform, which works based on several algorithms. For the normal operation of SIMS analysis, several constraints were integrated into it. First, the signal component spectra on the frequency scale were described by a bi-parametric log-normal function whose parameters were maximum amplitude and maximum position (1).

$$\begin{cases} I(\nu) = I_m \cdot \exp\left\{ -\dfrac{\ln 2}{\ln^2 \rho} \cdot \ln^2\left(\dfrac{a-\nu}{a-\nu_m} \right) \right\} & (\text{at } \nu < a) \\ I(\nu) = 0 & (\text{at } \nu \geq a) \end{cases} \quad (1),$$

where I_m – intensity (max), v – wavenumber, ρ – band asymmetry parameter, α – function limiting point position (Hixon & Reshetnyak, 2009)

Further, it was considered that, regardless of the concentration of quenchers (natural in our case), the position of the spectral components does not change in any way, but only the signal intensity varies. These changes in amplitude are described by the Stern-Volmer law (2). The last delimitation was the increased number of analysed points relative to the desired parameters. This made it possible to reduce the effect of random noise.

$$\frac{F_0}{F} = \frac{\tau_0}{\tau} = 1 + K_{sv} \cdot c \quad (2),$$

where F_0, F – fluorescence intensity, τ_0, τ - lifetime (absence and presence of the quencher, respectively) K_{sv} – Sterm-Volmer constant (Hixon & Reshetnyak, 2009).

3.2. RESULTS

3.2.1. UV-VIS ABSORPTION SPECTROSCOPY MEASUREMENTS

The initial stage of each experiment was to check the absorption spectrum of the sample. Before measuring the sample itself, a buffer was prepared (described in 2.1. Materials section). The cuvette was subjected to intensive cleaning from dust and other components to reduce the effect of the peripheral signal. First, the absorption spectra of a clean cuvette with buffer were measured. In the case of a successful result (minimum buffer signal in the UV region), samples were added, and their absorption spectrum was also measured. Since the number and position of Trp molecules, as well as other amino acid residues (inc. Tyr and Phe), differ in LH complexes derived from different purple bacteria, and the signal contribution depends on the natural quenching, the absorption spectra vary in shape (Figure 14). These measurements allow us to understand the component content of the LH complexes understudy on a broad spectral range (from 200 nm to 1000 nm). The well-marked peaks in the range from 780 to 880 nm (near-infrared) show the behaviour of bacteriochlorophylls. In comparison, the absorption signal in the range of approximately 420 to 580 nm belongs to carotenoids. The protein signal is located in the UV range of the spectra, and the absorption peak for them is located at approximately 280 nm.

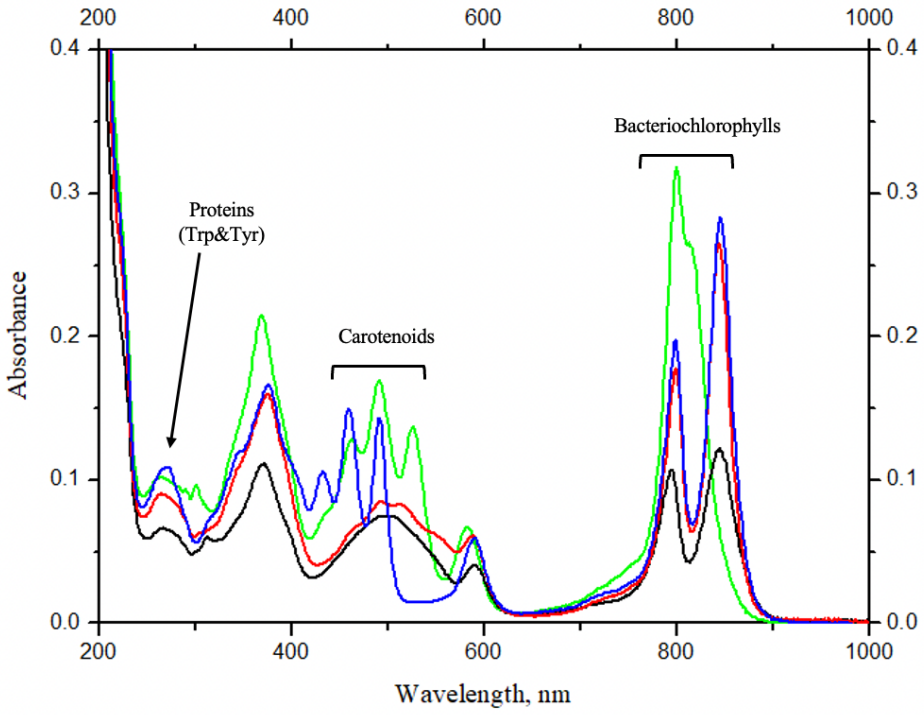

Figure 14. Absorption spectra for different bacteria (red – LH2 from *Rba. sphaeroides* (WT), green – LH3 from *R. acidophilus* (WT), blue – LH2 from *Rba. sphaeroides* (CrtC$^-$ mutant) and black – LH2 from *E. haloalkliphila* (WT))

3.2.2. EMISSION SPECTRA OF LH2 COMPLEXES FROM DIFFERENT BACTERIA

After absorption, the sample was placed in a spectrometer, where its fluorescence spectrum was measured. Excitation wavelengths in the UV region were selected in the range from 210 nm to 300 nm with a measurement step of 2 nm, since Trp produces visible fluorescence in this range. The process was controlled from a computer using the Andor Solis and Chirascan Windows programs, which made it possible to quickly change the measurement parameters and monitor the result in real-time. In the early stages of the study, a filter with a transmission capacity above 300 nm was used to exclude spectral noise such as Raman scattering. However, the filter had an influence on the essential Trp fluorescence signal, which made it difficult to understand the spectral interaction between two neighbouring amino acid residues. All final received data were measured without using any filters.

The main settings of the system during the operation were the choice of the spectral region, the use of an accumulation time of 20 s and a slit width of 2 nm. An example of the Trp emission spectra for an LH2 sample from *Rba. spheroides (*CrtC$^-$ mutant*)* are presented in Figure 15a and a comparison of fluorescence for different bacteria is shown in Figure 15b. The signal has been normalised excluding the buffer signal and the device's sensitivity. Similar spectra for all samples were used for further analysis.

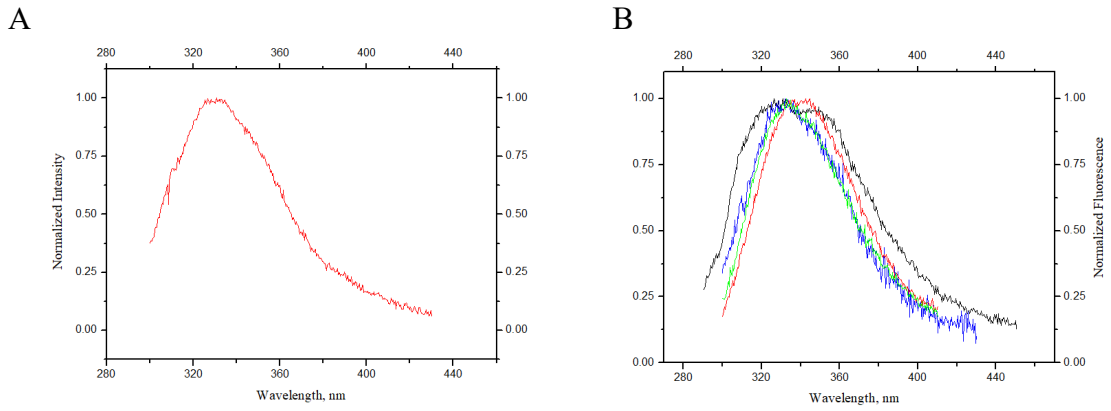

Figure 15. Normalised fluorescence spectra. The x-axis shows the wavelength of the excitation spectrum, and the y-axis shows the signal intensity; A. The emission spectrum of Trp (LH2 *Rba. spheroides* CrtC$^-$ mutant) excited at 280 nm; B. The emission spectra of Trp from different bacteria (red – LH2 from *Rba. sphaeroides* (WT*)*, green – LH3 from *R. acidophilus* (WT), blue – LH2 from *Rba. sphaeroides* (CrtC$^-$ mutant) and black – LH2 from *E. haloalkliphila* (WT)) excited at 250 nm

3.2.3. FLUORESCENCE CORRELATION ANALYSIS USING PFAST

Next, the decomposition analysis of Trp fluorescence with a priority on dividing the signal into two components was performed. For this, emission signals corrected for the buffer signal and device sensitivity were used, as mentioned earlier (described in 3.2.2. Emission spectra of LH2 complexes from different bacteria). The fluorescence spectrum of pure Trp, was measured at the same system settings as the Trp in LH complexes at an excitation wavelength of 297 nm (since mainly the tryptophan signal can be measured in proteins only in the range from 295 nm to 305 nm). Also, this parameter served as input data for the PFAST to create a correction curve. As the outcome, we obtained the classification of various Trp groups into spectral classes. The decision that the separation into two components is the most accurate representation was made based on data that showed the smallest percentage of the decomposition error (Figure 16 and Table 4). This remark is valid for all samples, making the further comparison more objective.

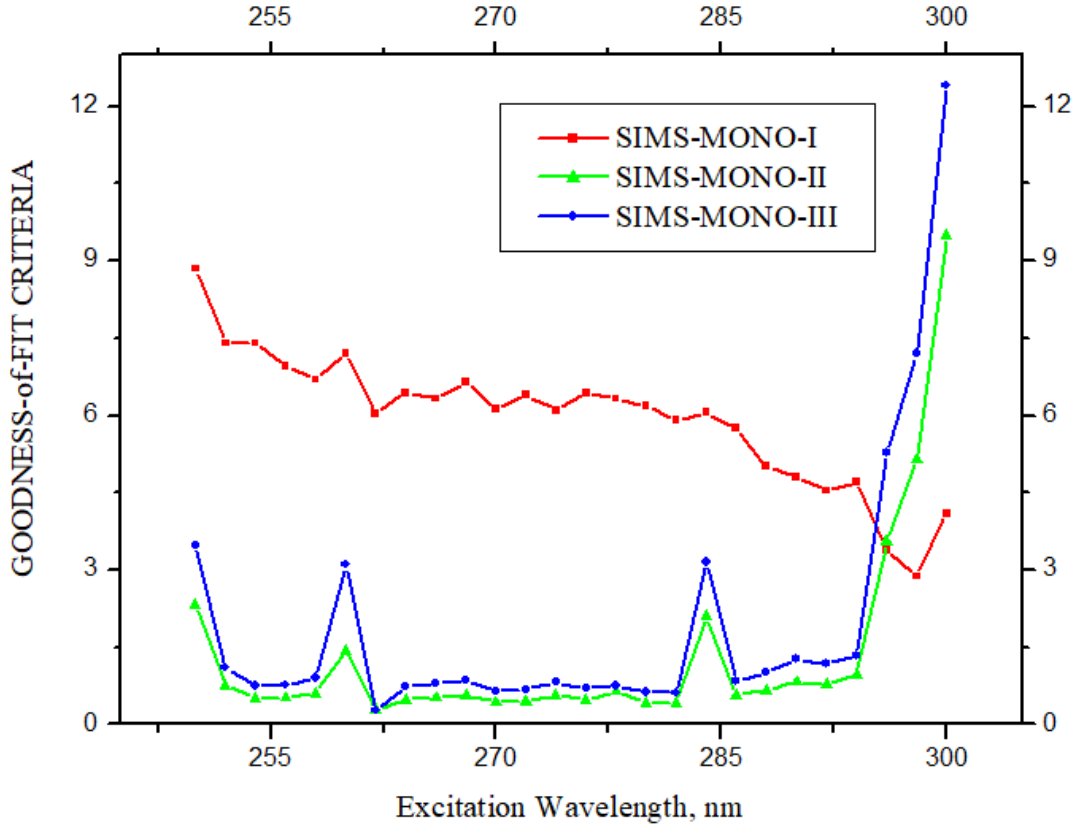

Figure 16. A comparison of the quality parameter within three analyses in the spectral region of excitation wavelength between 250 nm and 300 nm for the LH2. *Rba. sphaeroides* ($CrtC^-$ mutant) sample. Decomposition analysis into one, two and three components are marked with red, green, and blue lines, respectively. The y -axis is the goodness-of-fit criteria (DISCR.), and on the x-axis excitation wavelength (nm) is shown

The decomposed theoretical signal is slightly shifted in comparison with the original data. This can be explained by the Tyr contribution to the overall signal. Visual representation of the spectral position of the Trp signal in LH complexes compared to the signal of its pure form (L-Trp) in solution is shown in Figure 17.

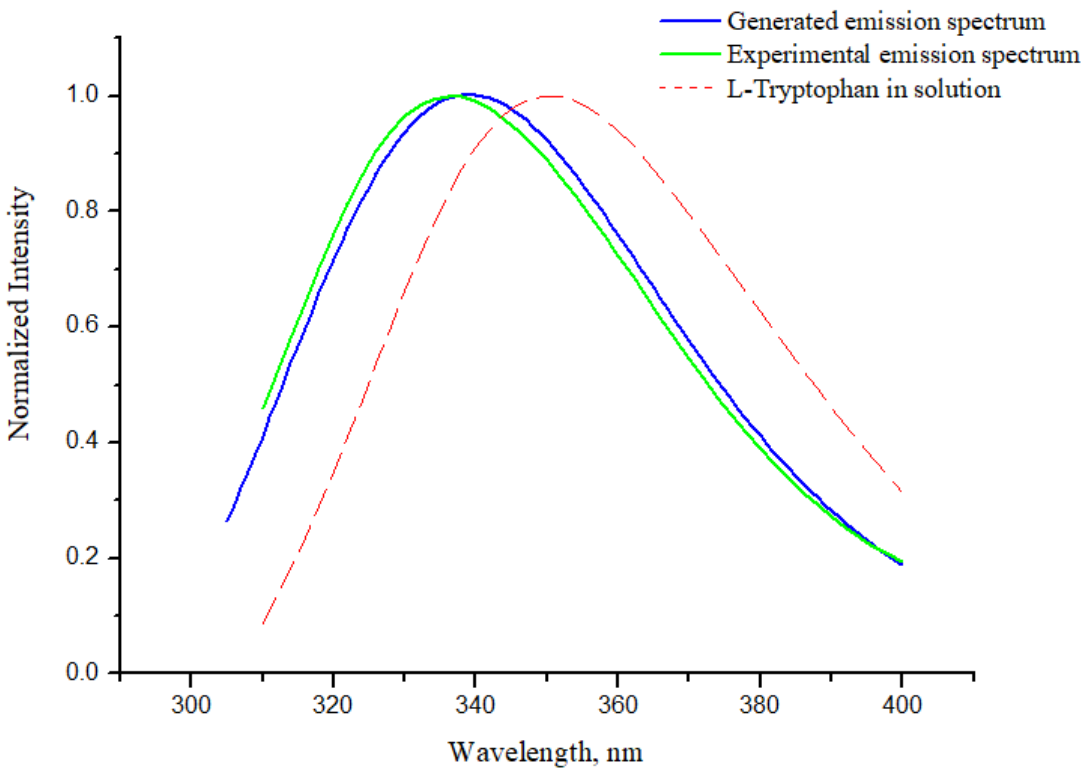

Figure 17. Trp fluorescence from the LH3 complex (*R. acidophilus*) excited at 280 nm. The redshift of the emission spectrum generated by PFAST after normalising it to the Tyr signal is shown. The green line represents the graph of the measured data, while the blue line is the result obtained after running the program. The red dashed curve is the fluorescence spectrum of pure Trp in solution, which was used as a correction curve. The y-axis shows the intensity of fluorescence, while the x-axis is emission wavelength (nm)

By visual comparison, it can be observed that tryptophan residues of different positions would have other effects on the overall fluorescence spectrum (Figure 18). It is important to note that the results depicted here show the state of affairs only in the case of an excitation wavelength of 268 nm for all samples. This wavelength was chosen randomly, and the ratio of the first and second components are changing among excitation spectra.

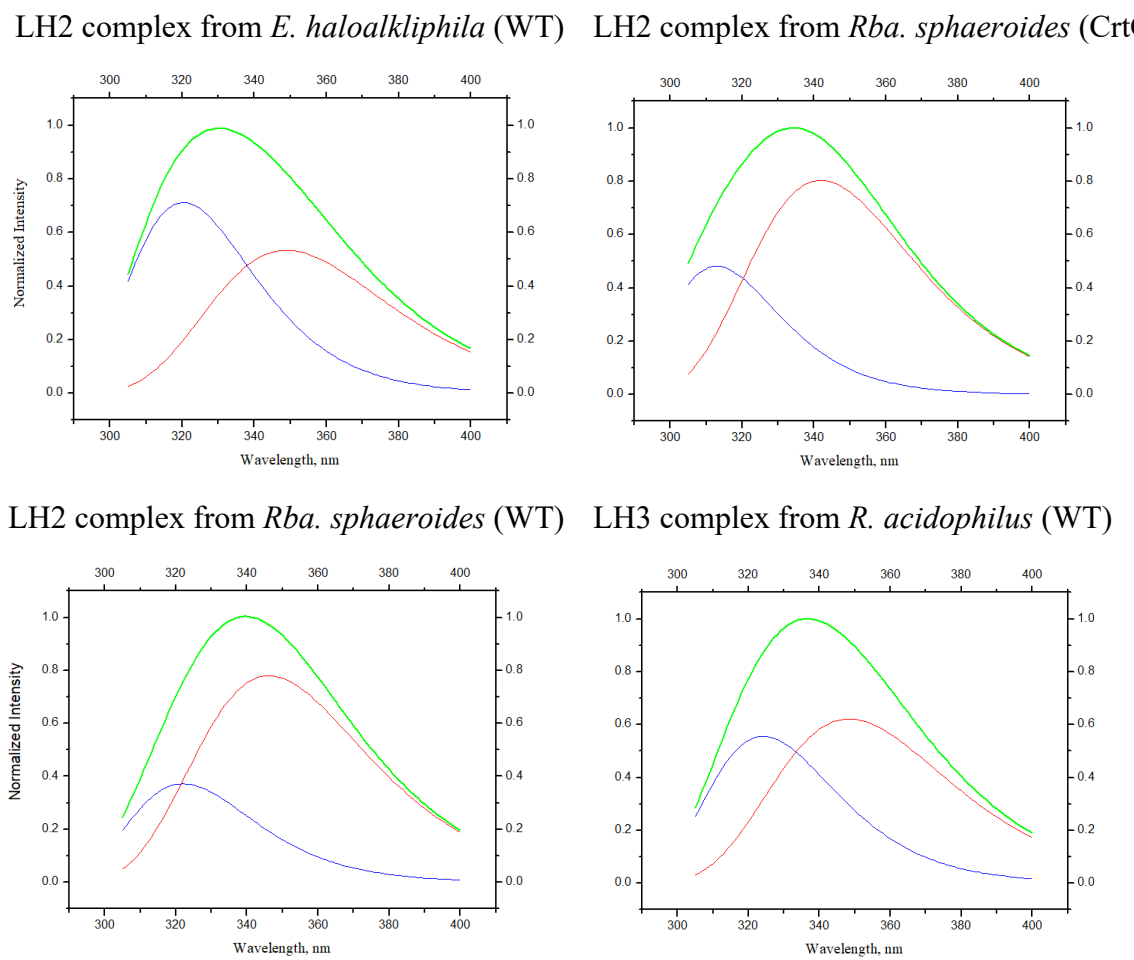

Figure 18. SIMS-MONO-II analysis for different samples. The green line shows the tyrosine-corrected fluorescence spectrum (theoretical spectrum) measured at an excitation wavelength of 268 nm for all samples. The blue line represents the first component (presumably located closer to the N-terminal), while the red line represents the second analysis component (located in the C-terminal)

In addition to the graphical data, the output of the analysis also contains data on the maximum position of the spectral components indicated in wavelength (nm) and the number of waves (1^{-} ^{cm}), as well as the contribution of each component in the theoretical spectrum, the standard deviation and the areas covered by each spectral graph. An example of a summary analysis table is listed below (Table 4).

The emission spectrum of Trp from the LH2 complex (*Rba. sphaeroides* $CrtC^{-}$ mutant) was used as an example corresponding to an excitation wavelength equal to 276 nm. As can be seen from the second column, and as noted earlier, the two-component analysis has the lowest DISCR., making it the most reliable. The distribution of spectral components by class is shown in the last column in Table 4. A detailed description of the spectral types is presented in Table S1.

Table 4. Summary result of decomposition from Fluorescence correlation analysis (PFAST)

PROGRAMM	DISCR.	Nsc	N	Lm,nm	S,%	CLASS
SIMS - 1	6.437	7	1	336.7 +/- 0.5	100 +/- 0	I or II
SIMS - 2	0.478	0	1	312.7 +/- 0.5	34 +/- 1	A
			2	341.2 +/- 0.5	66 +/- 1	II
SIMS - 3	0.702	0	1	313.1 +/- 1	34.1 +/- 8	A
			2	321.3 +/- 15.5	0.1 +/- 2387	S
			3	341.3 +/- 0.5	65.8 +/- 4	II

DISCR. - Goodnes-of-Fit. (average error of decomposition)
Nsc - Number of smoothed cycles
N - Number of spectral components
Lm - Maximum position of spectral components in nm
S,% - Contribution of spectral components in total spectrum in %
Class - Assignemnet of spectral components to spectral classes

After obtaining data from all areas in the studied range, a characteristic was made by the main spectral parameters on the energy scale. Indicators such as the position of the maximum peak, the width of the spectra and the maximum intensity, were visualised on different graphs separately for the first and second components. Each graph includes curve data for different samples (Figure 19). This was done to demonstrate the behaviour of the tryptophan spectrum depending on its position in the protein complex.

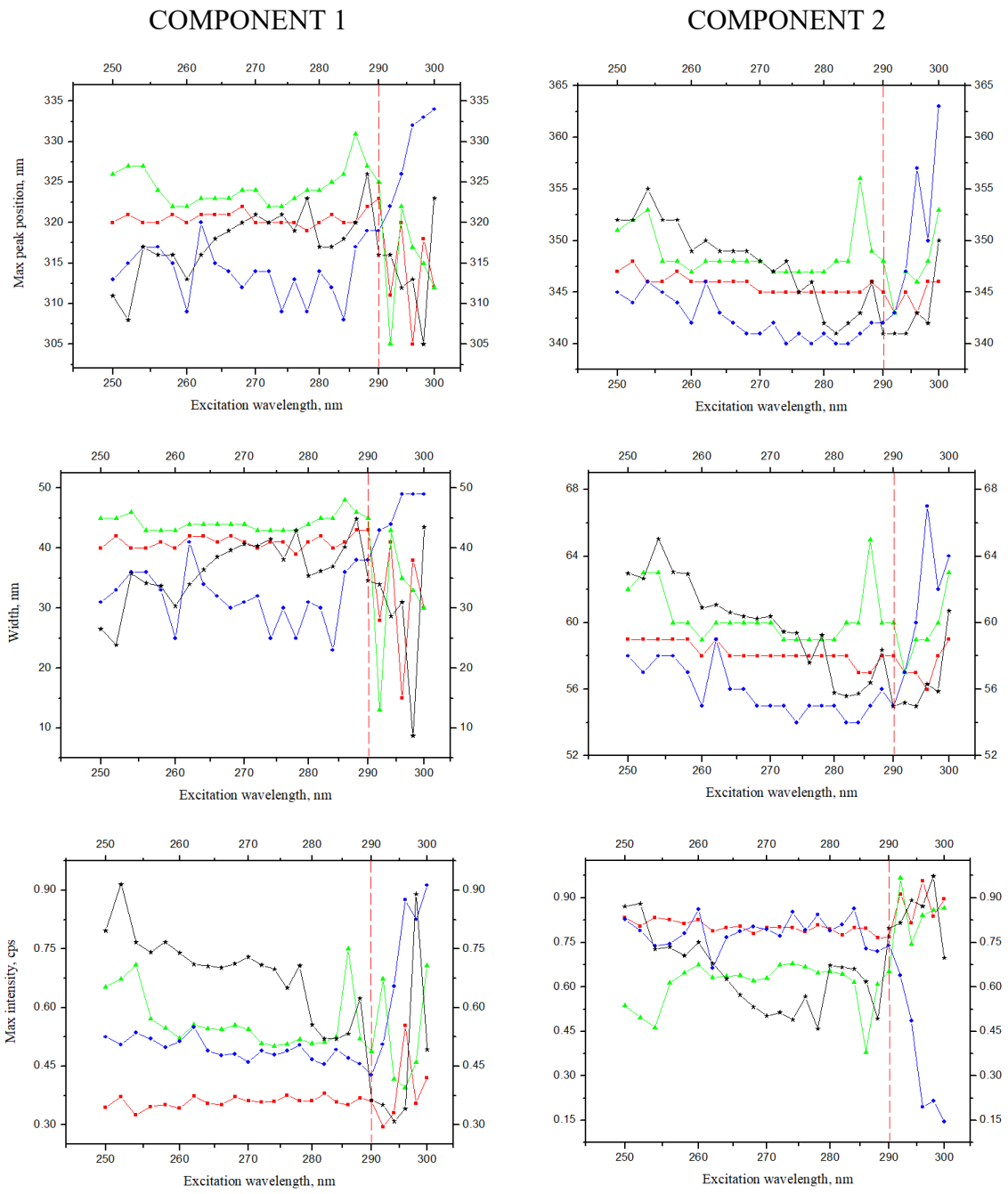

Figure 19. The comparative dependence of the main characteristics of the spectral signal for different samples (red – LH2 from *Rba. sphaeroides* (WT), green – LH3 from *R. acidophilus* (WT), blue – LH2 from *Rba. sphaeroides* ($CrtC^-$ mutant) and black – LH2 from *E. haloalkliphila* (WT)) on the excitation wavelength. Decomposition analysis (left) is the characteristics of the fluorescence spectrum of the first component, while the graphs on the right are responsible for the second component of the decomposition analysis. The red dashed line divides the graphs into two parts, the right part of which has a higher noise value and deviates from the general trend

3.3. DISCUSSION

The behaviour of individual tryptophan residues signal in membrane proteins of photosynthetic complexes is currently an unexplored topic, but new discoveries in the field of proteomics have become the starting point for studying this issue (Peak et al., 1983). Various spectral analytical methods were used in the course of this work, however, due to the complex behaviour of the Trp signal, the study of the simulated results became a paramount issue.

Comparison of absorption curves for different light-harvesting complexes of different bacteria gave a clearer understanding of the amount and position of the components in photosynthetic complexes. Based on a combination of the data obtained with already existing absorption curves of LH complexes, the spectral position of the components in both the UV and near IR regions was confirmed (Figure 14) (Niedzwiedzki et al., 2012, 2017). Nevertheless, spectral analysis of LH in the region of 300 nm is optimal for comparing the behaviour of proteins and bacteriochlorophylls in complexes. Noticeable differences in the fluorescence spectra were recorded for different bacterial cells (Figure 15b).

At the initial stage of work, the possibility of using the open-source platform PFAST and its integration into work was completely unpredictable. The reason for this was that the database was created for globular proteins and did not include transmembrane complexes (Reshetnyak et al., 2001; Reshetnyak & Burstein, 1977). Due to the unique structure of membrane proteins, they did not need the addition of quenchers, as they had a similar natural effect. Another aspect that makes this platform not entirely suitable for detailed analysis is its tendency to use a sufficiently large step relative to the spectral data, allowing it to work with at least 1 nm. This is enough to give a first impression of the behaviour of the signal but at the same time a lower resolution analysis in relation to the main spectral characteristics, which are clearly visible in the red line in Figure 19 (upper right graph). Also, a rather high analysis error was noticed in comparing the data measured at different excitation wavelengths. This made it necessary to repeat one analysis several times until relatively satisfactory results were obtained. However, as can be seen from the graphs in Figure 19, the parts to the right of the red dashed line have a large effect of noise and give a relatively high DISCR. value (Figure 16).

Despite all listed above, PFAST gave a visual representation of the spectral components' contribution and dependency on Trp positions in the protein structure. The correspondence of the data in terms of the spectral position of the components was confirmed by the example of

the Trp fluorescence signal from the bacterium *E. haloalkliphila* since there was initially the most noticeable presence of two different structures.

It was ideal to divide the tryptophan fluorescence signal into several components equal to the amount of tryptophan residue in the structure of the transmembrane helix since each molecule contributes to the final signal (Vivian & Callis, 2001). However, this work is complicated due to the strong overlap of signals from nearby amino acids, available and used equipment. In this regard, we decided to divide the signal into two parts corresponding to the C- and N- terminal parts of the protein structure. The amount of Trp varied among the samples, which also influenced the results. Despite the difference in spectral characteristics, the overall signal dependence for the three samples is approximately the same, while in the case of the *E. haloalkliphila*, one can observe a different behaviour compared to others. This can be explained by Trp location, which is also noted in Table 3 (the Trp41 of the beta chain (hydropathy index 1.06), Trp27 in the alpha chain (hydropathy index 0.38) located closer to the membrane side, and Trp16 (hydropathy index -1.24) with the integrated position in the membrane part). The difference between the behaviour of the first components from *Rba. sphaeroides and Rba. sphaeroides* $CrtC^-$ mutant is presumably due to the presence of only neurosporene in the second case, which transmits the signal to the red-shift side, but the general trend of behaviour remains the same in both cases.

Conclusions made based on the obtained data confirm the dependence of the spectral signal on the position of Trp relative to the protein structure, however, need further detailed study.

SUMMARY

Despite the extensive knowledge of photosynthesis, many of its fundamental principles are still a mystery. Complexes isolated from the membranes of photosynthetic bacteria, in particular, bacteria with anoxygenic photosynthesis, are a promising material for studying biophysical processes. This group has a wide distribution, and basic photosynthetic cycles and is potentially helpful in researching more complex photosynthetic processes due to their evolutionary position.

In this work, various methods of spectral analysis were used to study light-harvesting complexes from various purple bacteria. We chose a tryptophan residue as the main fluorescent component of the protein molecule. The tryptophan fluorescence signals for various samples were processed and then integrated into the PFAST open-source program to study the behaviour and structure of various components of the photosynthetic complex. Based on the data obtained, the dependence of the main spectral characteristics on excitation was acquired. Having drawn an analogy of this dependence with the structural parameters of the studied proteins, it was found that Trp position affects the level of the luminescence signal. Thus, for example, Trp located in a more hydrophilic medium had a spectral behaviour trend different from others.

REFERENCES

Andy Freer, S. P. K. S. M. P. A. H.-L. G. M. R. C. and N. W. I. (1996). Pigment–pigment interactions and energy transfer in the antenna complex of the photosynthetic bacteriumRhodopseudomonas acidophila. *Structure*, *4*(4), 449–462.

Axelrod, H. L., & Okamura, M. Y. (2005). The structure and function of the cytochrome c 2 : reaction center electron transfer complex from Rhodobacter sphaeroides. In *Photosynthesis Research* (Vol. 85). Springer.

Blankenship, R. E., Sadekar, S., & Raymond, J. (2007). The Evolutionary Transition from Anoxygenic to Oxygenic Photosynthesis. In *Evolution of Primary Producers in the Sea*. https://doi.org/10.1016/B978-0-12-370518-1.50004-7

Brown, C. T., Hug, L. A., Thomas, B. C., Sharon, I., Castelle, C. J., Singh, A., Wilkins, M. J., Wrighton, K. C., Williams, K. H., & Banfield, J. F. (2015). Unusual biology across a group comprising more than 15% of domain Bacteria. *Nature*, *523*(7559), 208–211. https://doi.org/10.1038/nature14486

Castelle, C. J., & Banfield, J. F. (2018). Major New Microbial Groups Expand Diversity and Alter our Understanding of the Tree of Life. In *Cell* (Vol. 172, Issue 6, pp. 1181–1197). Cell Press. https://doi.org/10.1016/j.cell.2018.02.016

Chen, Y., & Barkley, M. D. (1998). *Toward Understanding Tryptophan Fluorescence in Proteins †*.

Cogdell, R. J., Gardiner, A. T., Roszak, A. W., Law, C. J., Southall, J., & Isaacs, N. W. (2004). *Rings, ellipses and horseshoes: how purple bacteria harvest solar energy*.

Determine Protein Concentration Using Microvolumes with the Agilent Cary 60 UV-Vis Spectrophotometer. (2022). www.agilent.com/chem/cary60

Ferretti, M., Hendrikx, R., Romero, E., Southall, J., Cogdell, R. J., Novoderezhkin, V. I., Scholes, G. D., & van Grondelle, R. (2016). Dark States in the Light-Harvesting complex 2 Revealed by Two-dimensional Electronic Spectroscopy. *Scientific Reports*, *6*. https://doi.org/10.1038/srep20834

Fiedor, L., Kania, A., Myśliwa-Kurdziel, B., Orzeł, Ł., & Stochel, G. (2008). Understanding chlorophylls: Central magnesium ion and phytyl as structural determinants. *Biochimica et*

Biophysica Acta - Bioenergetics, *1777*(12), 1491–1500. https://doi.org/10.1016/j.bbabio.2008.09.005

Forester T. (1948). Zwischenmolekulare Energiewanderung and Fluoreszenz. *Annalen Der Physil*, *6*(2), 55–75.

Francia, F., Dezi, M., Rebecchi, A., Mallardi, A., Palazzo, G., Melandri, B. A., & Venturoli, G. (2004). Light-harvesting complex 1 stabilizes P+QB- charge separation in reaction centers of Rhodobacter sphaeroides. *Biochemistry*, *43*(44), 14199–14210. https://doi.org/10.1021/bi048629s

Galili, G., Avin-Wittenberg, T., Angelovici, R., & Fernie, A. R. (2014). The role of photosynthesis and amino acid metabolism in the energy status during seed development. *Frontiers in Plant Science*, *5*. https://doi.org/10.3389/fpls.2014.00447

Hamilton, T. L. (2019). The trouble with oxygen: The ecophysiology of extant phototrophs and implications for the evolution of oxygenic photosynthesis. In *Free Radical Biology and Medicine* (Vol. 140, pp. 233–249). Elsevier Inc. https://doi.org/10.1016/j.freeradbiomed.2019.05.003

Hansen, J., Nazarenko, L., Ruedy, R., Sato, M., Willis, J., Genio, A. del, Koch, D., Lacis, A., Lo, K., Menon, S., Novakov, T., Perlwitz, J., Russell, G., Schmidt, G. A., & Tausnev, N. (2005). Earth's Energy Imbalance: Confirmation and Implications. *Science*, *308*, 1431–1435. www.sciencemag.org

Hill, N. C., Tay, J. W., Altus, S., Bortz, D. M., & Cameron, J. C. (2020). *Life cycle of a cyanobacterial carboxysome*. https://www.science.org

Hixon, J., & Reshetnyak, Y. K. (2009). Algorithm for the analysis of tryptophan fluorescence spectra and their correlation with protein structural parameters. In *Algorithms* (Vol. 2, Issue 3, pp. 1155–1176). https://doi.org/10.3390/a2031155

Hu, X., Damjanovic´, A. D., Ritz, T., & Schulten, K. (1998). Architecture and mechanism of the light-harvesting apparatus of purple bacteria. In *Computational Biomolecular Science* (Vol. 95). www.pnas.org.

Jones, C. S., & Mayfield, S. P. (2012). Algae biofuels: Versatility for the future of bioenergy. In *Current Opinion in Biotechnology* (Vol. 23, Issue 3, pp. 346–351). https://doi.org/10.1016/j.copbio.2011.10.013

Jones, M. R., Fowler, G. J. S., Gibson, L. C. D., Grief, G. G., Olsen, J. D., Crielaard^, W., & Hunter, C. N. (1992). Mutants of Rhodobacter sphaeroides lacking one or more pigment-protein complexes and complementation with reaction-centre, LH1, and LH2 genes. In *Molecular Microbiology* (Vol. 6, Issue 9).

Kumar Maurya, P., Mondal, S., Kumar, V., & Singh, S. P. (2021). Roadmap to sustainable carbon-neutral energy and environment: can we cross the barrier of biomass productivity? *Environmental Science and Pollution Research* , *28*, 49327–49342. https://doi.org/10.1007/s11356-021-15540-8/Published

Lakowicz, J. R. (2006). *Principles of Fluorescence Spectroscopy Third Edition*.

Law, C. J., Roszak, A. W., Southall, J., Gardiner, A. T., Isaacs, N. W., & Cogdell, R. J. (2004). The structure and function of bacterial light-harvesting complexes. In *Molecular Membrane Biology* (Vol. 21, Issue 3, pp. 183–191). https://doi.org/10.1080/09687680410001697224

Madigan, M. T., & Jung, D. O. (2009). *An Overview of Purple Bacteria: Systematics, Physiology, and Habitats* (pp. 1–15). https://doi.org/10.1007/978-1-4020-8815-5_1

McLuskey, K., Prince, S. M., Cogdell, R. J., & Isaacs, N. W. (2001). The crystallographic structure of the B800-820 LH3 light-harvesting complex from the purple bacteria Rhodopseudomonas acidophila strain 7050. *Biochemistry*, *40*(30), 8783–8789. https://doi.org/10.1021/bi010309a

Milukov A., P. C. , J. B. (2007). Spectroscopic study of a culture of purple sulfur bacteria Chromatium sp. in the aquatic environment. *Bulletin of Moscow University*, *3*, 40–43.

Montalti, M., Credi, A., Prodi, L., Gandolfi, M. T., Michl, J., & Balzani, V. (2006). *Handbook of photochemistry*.

Niederman, R. A. (2017). Photosynthesis in the purple bacteria. In *Modern Topics in the Phototrophic Prokaryotes: Metabolism, Bioenergetics, and Omics* (pp. 193–224). Springer International Publishing. https://doi.org/10.1007/978-3-319-51365-2_6

Niedzwiedzki, D. M., Bina, D., Picken, N., Honkanen, S., Blankenship, R. E., Holten, D., & Cogdell, R. J. (2012). Spectroscopic studies of two spectral variants of light-harvesting complex 2 (LH2) from the photosynthetic purple sulfur bacterium Allochromatium vinosum. *Biochimica et Biophysica Acta - Bioenergetics*, *1817*(9), 1576–1587. https://doi.org/10.1016/j.bbabio.2012.05.009

Niedzwiedzki, D. M., Dilbeck, P. L., Tang, Q., Martin, E. C., Bocian, D. F., Hunter, C. N., & Holten, D. (2017). New insights into the photochemistry of carotenoid spheroidenone in light-harvesting complex 2 from the purple bacterium Rhodobacter sphaeroides. *Photosynthesis Research*, *131*(3), 291–304. https://doi.org/10.1007/s11120-016-0322-2

Ogata, S. (1964). *The mechanism of photosynthesis in purple sulfur bacteria*.

Papiz, M. Z., Prince, S. M., Howard, T., Cogdell, R. J., & Isaacs, N. W. (2003). The structure and thermal motion of the B800-850 LH2 complex from Rps. acidophila at 2.0 Å resolution and 100 K: New structural features and functionally relevant motions. *Journal of Molecular Biology*, *326*(5), 1523–1538. https://doi.org/10.1016/S0022-2836(03)00024-X

Peak, D., Werner, T. C., Dennin, R. M., & Baird, J. K. (1983). *Fluorescence quenching at high quencher concentrations*.

Philippi, M., Kitzinger, K., Berg, J. S., Tschitschko, B., Kidane, A. T., Littmann, S., Marchant, H. K., Storelli, N., Winkel, L. H. E., Schubert, C. J., Mohr, W., & Kuypers, M. M. M. (2021). Purple sulfur bacteria fix N2 via molybdenum-nitrogenase in a low molybdenum Proterozoic ocean analogue. *Nature Communications*, *12*(1). https://doi.org/10.1038/s41467-021-25000-z

Reddy, A. R., Rasineni, G. K., & Raghavendra, A. S. (2010). The impact of global elevated CO 2 concentration on photosynthesis and plant productivity †. In *CURRENT SCIENCE* (Vol. 99, Issue 1).

Reinbothe, S., & Reinbothe, C. (1996). Evolution of Chlorophyll Minireview Biosynthesis-The Challenge to Survive Photooxidation. In *Cell* (Vol. 86).

Reshetnyak, Y. K., & Burstein, E. A. (1977). Intrinsic Protein Luminescence (The Nature and Application). In *Itogi Nauki i Tekhniki), Biophysics* (Vol. 18). VINITI.

Reshetnyak, Y. K., Koshevnik, Y., & Burstein, E. A. (2001). *Decomposition of Protein Tryptophan Fluorescence Spectra into Log-Normal Components. III. Correlation between Fluorescence and Microenvironment Parameters of Individual Tryptophan Residues*.

Roszak, A. W., Howard, T. D., Southall, J., Gardiner, A. T., Law, C. J., Isaacs, N. W., & Cogdell, R. J. (2003). Crystal Structure of the RC-LH1 Core Complex from Rhodopseudomonas palustris. *Science*, *302*(5652), 1969–1972. https://doi.org/10.1126/science.1088892

Royer, C. A. (1995). *Fluorescence Spectroscopy*.

Sadi, N. H., & Firmansyah, F. (2020). The Potency of Purple Sulphur Bacteria for In-Situ Sulphide Bioremediation in Water. *IOP Conference Series: Earth and Environmental Science*, *477*(1). https://doi.org/10.1088/1755-1315/477/1/012002

Saer, R. G., & Blankenship, R. E. (2017). Light harvesting in phototrophic bacteria: Structure and function. *Biochemical Journal*, *474*(13), 2107–2131. https://doi.org/10.1042/BCJ20160753

Scheuring, S., Rô Me Seguin, J., Marco, S., Lé, D., Robert, B., & Rigaud, J.-L. (2002). *Nanodissection and high-resolution imaging of the Rhodopseudomonas viridis photosynthetic core complex in native membranes by AFM*. www.pnas.orgcgidoi10.1073pnas.0437992100

Serrano-Ruiz, J. C., & Dumesic, J. A. (2011). Catalytic routes for the conversion of biomass into liquid hydrocarbon transportation fuels. *Energy and Environmental Science*, *4*(1), 83–99. https://doi.org/10.1039/c0ee00436g

Siebert, C. A., Qian, P., Fotiadis, D., Engel, A., Hunter, C. N., & Bullough, P. A. (2004). Molecular architecture of photosynthetic membranes in Rhodobacter sphaeroides: The role of PufX. *EMBO Journal*, *23*(4), 690–700. https://doi.org/10.1038/sj.emboj.7600092

Sípoš, R. R. ˇ, & Sima, J. ˇ. (2020). JABLONSKI DIAGRAM REVISITED. In *Rev. Cubana Fis* (Vol. 37).

Smashevsky N. (2014). Ecology of Photosynthesis. *ASTRAKHAN BULLETIN OF ENVIRONMENTAL EDUCATION*, *2*(28), 165–180.

Stirbet, A., Lazár, D., Guo, Y., & Govindjee, G. (2020). Photosynthesis: Basics, history and modelling. In *Annals of Botany* (Vol. 126, Issue 4, pp. 511–537). Oxford University Press. https://doi.org/10.1093/aob/mcz171

Tani, K., Nagashima, K. V. P., Kanno, R., Kawamura, S., Kikuchi, R., Hall, M., Yu, L. J., Kimura, Y., Madigan, M. T., Mizoguchi, A., Humbel, B. M., & Wang-Otomo, Z. Y. (2021). A previously unrecognized membrane protein in the Rhodobacter sphaeroides LH1-RC photocomplex. *Nature Communications*, *12*(1). https://doi.org/10.1038/s41467-021-26561-9

This guide provides a technical description of the Chirascan-plus CD Spectrometer. (2008). www.photophysics.com

Timpmann, K., Linnanto, J. M., Yadav, D., Kangur, L., & Freiberg, A. (2021). Hydrostatic High-Pressure-Induced Denaturation of LH2 Membrane Proteins. *Journal of Physical Chemistry B*, *125*(35), 9979–9989. https://doi.org/10.1021/acs.jpcb.1c05789

van Amerongen, H., & van Grondelle, R. (2001). Understanding the energy transfer function of LHCII, the major light-harvesting complex of green plants. *Journal of Physical Chemistry B*, *105*(3), 604–617. https://doi.org/10.1021/jp0028406

Vivian, J. T., & Callis, P. R. (2001). Mechanisms of tryptophan fluorescence shifts in proteins. *Biophysical Journal*, *80*(5), 2093–2109. https://doi.org/10.1016/S0006-3495(01)76183-8

APPENDIX 1

Table S1. Trp spectaral classes (Reshetnyak et al., 2001)

Spectral and structural parameters	Class A	Class S	Class I	Class II	Class III
The wavelengths of the most probable spectral positions (nm) revealed from an analysis of the fluorescence spectra of 160 proteins	308	321-325	330-333	341-344	346-350
Acc (averaged value of the relative solvent accessibility of the nine atoms of indole ring of the tryptophan fluorophore.)	1.9	0.81.4	6.0±3.6	14.8±7.5	55.3±15.9
Acc1-7 (averaged value of the relative solvent accessibility of 1 and 7 atoms of the tryptophan fluorophore)	0.0	1.0±2.2	11.2±8.5	26.7±19.1	71.1±19.5
Den (packing density: the number of neighbor atoms at a distance < 7.5 Å from the indole ring)	138.3	148.3±8.5	129.3±9.1	109.3±12.6	62.7±18.8
A (relative polarity of environment: portion of the atoms of the polar groups amongst all the atoms around the tryptophan residue at a distance < 7.5 Å)	23.5	34.5±5.8	39.3±5.5	45.1±7.4	65.5±13.9
B (B-factor: crystallographic B-factors of the atoms of the polar groups normalized to the mean B-factor value of all the Ca atoms in the crystal structure)	0.61	0.89±0.17	1.11±0.20	1.23±0.32	1.54±0.55
(Dynamic accessibility [R = Acc.B], a dynamic characteristic of the microenvironment)	0.9	0.7±1.2	6.7±4.0	18.2±10.3	85.2±30.9

NON-EXCLUSIVE LICENCE TO REPRODUCE THE THESIS

AND MAKE THE THESIS PUBLIC

I, Ali Jafarov,

1. grant the University of Tartu a free permit (non-exclusive licence) to:

reproduce, for the purpose of preservation, including for adding to the DSpace digital archives until the expiry of the term of copyright, my thesis

Spectroscopy of photosynthetic pigment-protein complexes from far-ultraviolet to near-infrared

supervised by Ass. Prof. Kõu Timpmann and Prof. Arvi Freiberg

2. I grant the University of Tartu the permit to make the thesis specified in point 1 available to the public via the web environment of the University of Tartu, including via the DSpace digital archives, under the Creative Commons licence CC BY NC ND 4.0, which allows, by giving appropriate credit to the author, to reproduce, distribute the work and communicate it to the public, and prohibits the creation of derivative works and any commercial use of the work from ***27/05/2022*** until the expiry of the term of copyright,
3. I am aware that the author retains the rights specified in points 1 and 2.

4. I confirm that granting the non-exclusive licence does not infringe other persons' intellectual property rights or rights arising from the personal data protection legislation.

Ali Jafarov

27/05/2022